EXHIBIT A

IN THE UNITED STATES DISTRICT COURT
FOR THE DISTRICT OF DELAWARE

In re Entresto (Sacubitril/Valsartan) Patent Litigation	C.A. No. 20-md-2930-RGA FILED UNDER SEAL
NOVARTIS PHARMACEUTICALS CORPORATION, Plaintiff, v. MSN PHARMACEUTICALS INC., MSN LABORATORIES PRIVATE LIMITED, MSN LIFE SCIENCES PRIVATE LIMITED, GERBERA THERAPEUTICS, INC., NANJING NORATECH PHARMACEUTICAL CO., LIMITED, Defendants.	C.A. No. 22-cv-1395-RGA FILED UNDER SEAL

RESPONSIVE EXPERT DECLARATION OF DR. RICHARD L. MCCREERY, PH.D.

the two spectra would be much more significant, observable, and consistent with spectra depicted in scientific literature that Dr. Park has cited and repeatedly relied on for her opinions. They are not. Indeed, the spectra are indistinguishable.

7. In view of at least the foregoing, it is my opinion that Dr. Park's Raman spectroscopy data cannot be used to show, demonstrate, or otherwise confirm that it is more likely than not that amorphous TVS as claimed is present in any accused product—including Defendants respective ANDA Products.

8. If asked to testify as an expert in this matter, I expect to testify regarding the issues, subject matter, data, and analysis set forth in this declaration, my rebuttal report, and any issues related thereto, including testimony rebutting the opinions lodged by experts retained by Novartis.

II. QUALIFICATIONS AND BACKGROUND

9. I received my B.S. in chemistry in 1970 from the University of California, Riverside, followed by my Ph.D. in analytical chemistry in 1974 from the University of Kansas. At the University of Kansas, I was awarded the National Science Foundation ("NSF") predoctoral fellowship for 1970-73.

10. I joined the Ohio State University ("OSU") as an Assistant Professor in 1974, where I was promoted to the position of Associate Professor in 1979 and full Professorship in 1983. At OSU, I was appointed the Dow Professor of Chemistry in 1998 and continued in that position till 2006. In 2006, I moved to the University of Alberta in Edmonton. My research group at the University of Alberta was part of a joint collaboration between the University and the Canadian National Institute of Nanotechnology. I retired from teaching in 2019 but maintained an active research group until 2023.

11. Over my research career spanning over 5 decades, my research group has

focused on Raman spectroscopy, electrochemistry, and molecular electronics. One of the primary tools used in my studies over the past decades is Raman spectroscopy. I would estimate that I have written over 80 articles involving Raman spectroscopy in peer-reviewed scientific journals.

12. I am also the author of the book titled "*Raman Spectroscopy for Chemical Analysis*" which was published by Wiley in 2000. This book discusses in detail, among other things, the fundamentals of Raman spectroscopy, instrumentation and its calibration, and the collection and analysis of Raman spectra. For example, my book devotes a chapter to calibration of Raman shifts, a topic that has been of vital interest to me. It has sold thousands of copies, can be found in every major University's library, and is a widely-used reference in the field.

13. Additionally, I led development of the ASTM standards (E 1840) for calibration of Raman shift values involving seven independent laboratories which determined 94 accurate Raman peak frequencies for 8 common chemicals, including the active ingredient of Tylenol. As listed in my resume, I have authored numerous research articles in Raman spectroscopy, including a study of 309 USP pharmaceutical standards in collaboration with the US FDA (*J. Pharm. Sci.* v. **87**, p.1,1998). Over the course of my research career, my estimate is that my research group and I have collected and analyzed over 100,000 Raman spectra. My group was the first to explore diode lasers, fiber optics and CCD detectors in Raman instrumentation, which led to the rapid rise of Raman spectroscopy in forensic and pharmaceutical analysis, including thousands of "hand-held" spectrometers used widely outside research labs.

14. My curriculum vitae describes my educational background and experience in

19. I understand that a POSA may have the combined understanding of those of ordinary skill in the various fields pertinent to the subject matter of a patent. Accordingly, a POSA may be an individual or a team of individuals.

20. In my opinion, a POSA with respect to the '918 patent would have had (1) a Ph.D. in chemistry or a related field; and (2) two or more years of experience with solid forms of pharmaceutical compounds, such as synthesizing, crystallizing, and characterizing solid forms of molecular pharmaceutical compounds, including experience in small-molecule characterization techniques (e.g., X-ray crystallography, Raman, etc.). Alternatively, a POSA could have had a less advanced degree in chemistry or a related field, with concomitantly more hands-on years of experience making and characterizing solid state pharmaceutical compounds. Furthermore, a POSA may have consulted with individuals having specialized expertise, for example, a clinician or practitioner with experience in the administration, dosing, and efficacy of medications for the treatment of hypertensive vascular diseases.

21. Plaintiff's expert, Dr. Park states that with regard to the '918 patent, Novartis's definition of a POSA is as follows:

> [A] person (or team) having ordinary skill in the art related to the '918 patent would have a Ph.D. or equivalent degree in chemistry or a related field and at least two years of experience with solid forms of molecular pharmaceutical compounds, including synthesis, crystallization, and characterization. Such a person or team having ordinary skill in the art could alternatively have less education and relatively more experience in the relevant areas. In addition, a person having ordinary skill in the art would have consulted with others having specialized knowledge, such as, for example, clinicians or medical doctors having experience administering, dosing, and evaluating the efficacy of medications for treating cardiovascular disease.

Park Decl. at ¶ 15.

22. I note that the foregoing definition of a POSA differs from the definition of

a POSA Dr. Park provided in her Opening Report, and it is unclear why Novartis has elected to alter its definition of a POSA. Nevertheless, and regardless of whether one of the foregoing definitions or a similar definition of a POSA is adopted, I exceed that level of education and experience, did so in 2005-2006, and was working in the relevant field before, during, and after 2005–2006 along with others who generally fit the foregoing description of a POSA. Thus, I am qualified to judge the capabilities and assess the perspective of a POSA under the above or any similar definition.

23. Regarding the legal principles used in my analysis, I am not a patent attorney, nor have I independently researched U.S. patent law. That said, I understand that I am obliged to follow existing U.S. patent law in rendering the opinions and analyses set forth in this report. Counsel has explained certain legal principles to me that I have relied on in forming my opinions and analyses. These legal principles are detailed at ¶¶ 15-21 of my Rebuttal Report. Ex. 2047.

24. I have given full consideration to, and have accounted for, the level of skill in the art relevant to this matter (again, which I exceed), in rendering my analysis and opinions, as well as the legal principles relevant to my analysis.

IV. THE '918 PATENT

25. The '918 patent is titled "AMORPHOUS SOLID FORM OF COMPOUNDS CONTAINING S-N-VALERYL-N-{[2'-(1H-TETRAZOLE-5-YL)-BIPHENYL-4-YL]- METHYL}-VALINE AND (2R,4S)-5-BIPHENYL-4-YL-4-(3-CARBOXYPROPIONYLAMINO)-2-METHYLPENTANOIC ACID ETHYL ESTER MOIETIES AND SODIUM CATIONS," and was issued on August 24, 2021. '918 patent, at cover. It lists Lili Feng et al. as inventors, and Novartis Pharmaceutical Corporation,

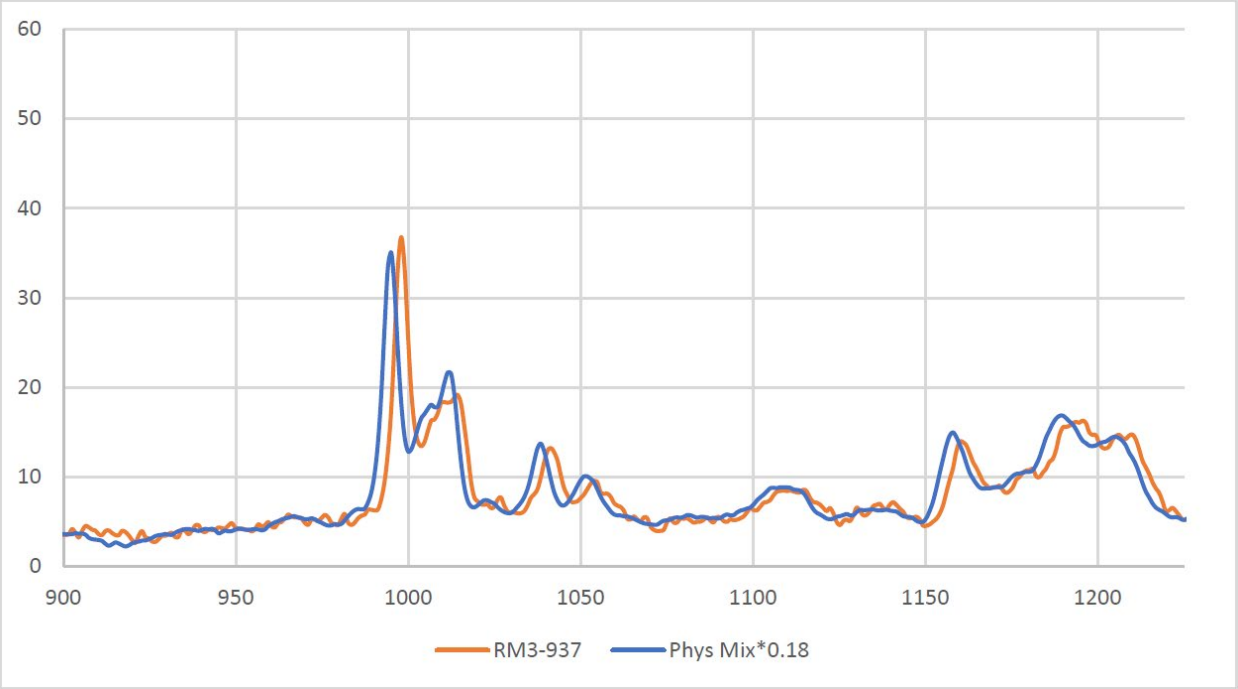

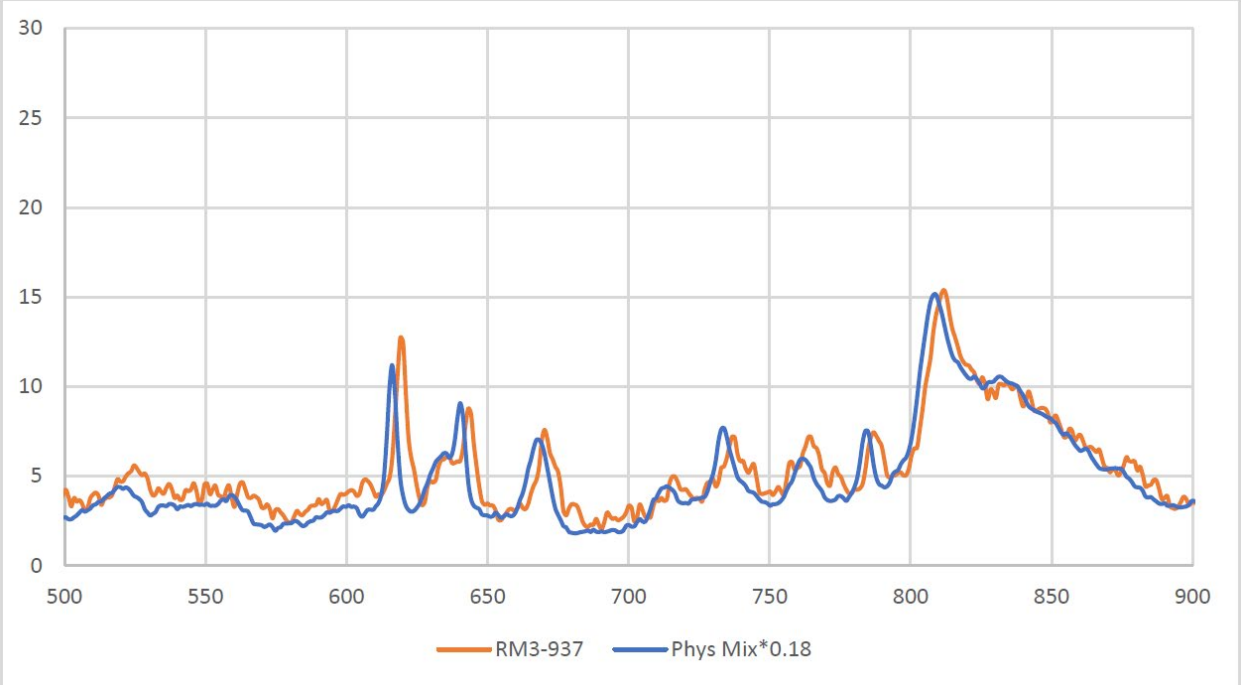

101. I observed that ***each peak corresponding to RM3-937*** (orange) was shifted by about 3 cm^{-1} towards the right (in this case, higher wave number), as compared to the Raman spectrum of the physical mixture. This phenomenon—i.e., ***every*** peak shifting in the ***same*** direction in roughly the ***same*** amount in Dr. Park's glassy solid spectrum when

compared with her physical mixture spectrum, is impossible if a new material, such as the claimed amorphous TVS, was actually formed. The supramolecular interactions claimed to exist in amorphous TVS must involve a few functional groups in a complex molecular structure, and would therefore affect some but not all of the frequencies observed in the spectrum. In contrast, ALL of the 20+ strongest peaks in the physical mixture spectrum are shifted by the same ~3 cm^{-1} amount. Indeed, in my five-plus decades of experience and my analysis of thousands of Raman spectra, I have never seen such universal shifting due to the formation of a new substance, nor would a scientist or POSA opine that such universal shifting is proof that a new substance was formed. Referring to the bond strengths as springs analogy discussed above, the 20+ uniform shifts apparent in Dr. Park's spectra would require *every* observed "spring" to increase in strength by the same amount in the glassy solid, which is chemically impossible.

102. In my opinion, the peak shifting that Dr. Park attributes to the formation of the purported "amorphous complex" is nothing but a calibration issue with her spectrometer. *First*, as mentioned above, if one were to rely on such a small Raman shift difference, a thorough calibration of the spectrometer with Raman or atomic emission standards needs to be performed prior to acquisition of the spectra. *Second*, if an amorphous complex were to form between the two drugs, the changes in the Raman spectra would not amount to a consistent shift by about 3 cm^{-1} to the right for all peaks. This is impossible. Instead, some peaks may shift while some may not. Some peaks may shift left (lower wavenumber as plotted) while others may shift towards the right (higher wavenumber as plotted). Some new peaks may appear while some others may not be observed in the "amorphous complex" compared to the individual components. The peaks that correspond to the bonds between

EXHIBIT B

IN THE UNITED STATES DISTRICT COURT
FOR THE DISTRICT OF DELAWARE

In re Entresto (Sacubitril/Valsartan) Patent Litigation — C.A. No. 20-2930-RGA

NOVARTIS PHARMACEUTICALS CORPORATION,

Plaintiff,

v. — C.A. No. 22-1395-RGA

MSN PHARMACEUTICALS INC., MSN LABORATORIES PRIVATE LIMITED, MSN LIFE SCIENCES PRIVATE LIMITED, GERBERA THERAPEUTICS, INC., NANJING NORATECH PHARMACEUTICAL CO., LIMITED,

Defendants.

REMOTE VIDEOTAPED DEPOSITION
OF
RICHARD L. McCREERY, Ph.D.

*** HIGHLY CONFIDENTIAL ***

Stenographically Reported By:
Amy L. Larson, RPR, CSR, CCR
Job No. J11739523

September 18, 2024
9:21 a.m. CST

Remote Videotaped Deposition of:

RICHARD L. McCREERY, Ph.D., taken before Amy L. Larson, a Registered Professional Reporter and Notary Public in the State of Minnesota, Notary Public in the State of Wisconsin, Certified Shorthand Reporter in the State of Illinois, Certified Court Reporter in the State of Washington, Certified Shorthand Reporter in the State of Oregon, Certified Court Reporter in the State of Utah, Certified Court Reporter in the State of New Mexico.

APPEARANCES:

Attorney for Plaintiff:
VENABLE LLP
151 West 42nd Street
New York, NY 10036
BY: CHRISTOPHER LOH, ESQ.
cloh@venable.com
CARRIE PARK, ESQ. (Chicago office)
cspark@venable.com
HUSCH BLACKWELL
120 South Riverside Plaza
Suite 2200
Chicago, IL 60606
BY: DON J. MIZERK, ESQ.
don.mizerk@huschblackwell.com

ALSO PRESENT:
Syed Rizvi
Brent Jordan, Videographer

INDEX:

MR. MIZERK: Objection. Instruct the witness not to answer. Rule 26 clearly does not allow this question.

BY MR. LOH:

Q. How much of that report did you write versus Husch Blackwell's lawyers?

MR. MIZERK: Objection. I'm going to instruct the witness not to answer. Chris, you know better, please --

BY MR. LOH:

Q. Are you going to follow that instruction?

THE COURT REPORTER: I'm sorry, I'm sorry, Mr. Mizerk, I didn't hear the last part of that.

MR. MIZERK: I said -- I think I said, "Chris, you know better."

And, yes, he is going to follow my instruction.

BY MR. LOH:

Q. How did you prepare for today's deposition?

A. How -- can you repeat the question?

Q. How did you prepare for today's deposition?

A. Prepare for today's deposition? Well, a lot of studying, reading of patents, talking to Husch Blackwell, doing some Excel work on the

spectra that we had to work with, doing a data analysis at a fairly high level given that I've done a lot of work with Raman spectroscopy, and I have made sure that I understood the story.

Q. Who did you meet with to prepare for today's deposition?

A. What?

Q. Who did you meet with to prepare for today's deposition?

A. Who did I meet with?

Q. Yes.

A. Don Mizerk and Syed Rizvi.

Q. And for how long did you meet with them?

A. All day yesterday in person, and we had a couple of Zoom meetings as well last week.

Q. If you could turn to the CV that's at the back of your report.

A. My CV?

Q. Yes.

A. Okay, I have it.

MR. MIZERK: And for the record, you're referring to Exhibit A of his report, Chris?

MR. LOH: Correct.

THE VIDEOGRAPHER: While we're doing that, Counsel, can you tilt -- or Mr. McCreery, can you tilt the camera up just a little bit, please? Just tilt it up.

THE WITNESS: Wrong way.

MR. MIZERK: Is that better or worse?

THE VIDEOGRAPHER: Well, he kind of came off. Recenter him back up in the frame.

THE WITNESS: It's the right altitude, but it needs a rotation. There you go.

BY MR. LOH:

Q. So the first page of your CV lists, "Research Interests."

Do you see that?

A. I see the first page, yes.

Q. And those research interests are surface spectroscopy, molecular electronics, electrochemical kinetics, and advanced carbon materials, correct?

A. Correct.

Q. Pharmaceutical compounds are not listed among your research interests; is that correct?

MR. MIZERK: Objection as to form. You can answer.

THE WITNESS: I don't -- pharmaceutical materials are not mentioned in those -- in that list, no.

BY MR. LOH:

Q. How much of your day-to-day work involves pharmaceutical compounds?

A. Repeat that, please.

Q. How much of your day-to-day work involves pharmaceutical compounds?

A. Well, we have a couple of papers about it. We did a drug study with the FDA where we did obtain spectra of 300 pharmaceutical USP standards. We have -- my original dozen papers were about chlorpromazine, which is the active ingredient of Thorazine.

I have several early papers in the Journal of Medicinal Chemistry. Probably the first ten years of my career was mainly on pharmaceutical materials, because my Ph.D. involved neurosciences, and I was interested in, particularly, heterocyclic antidepressants and antipsychotics.

So I can't give you a percentage. I

Page 21

can just tell you that I've been doing this for almost 50 years. I've had a lot of different things I've looked at, and many of them involve pharmaceuticals.
Q. Did the first ten years of your career involve the Raman spectroscopy?
A. Yes, it did. I started at Ohio State in 1974. I did a sabbatical in 1981 to the University of South Hampton and for the person who discovered surface-enhanced Raman, because I wanted to learn about surface spectroscopy mainly. So that would have been in '81.
So I bought my first Raman spectrometer about '83, so I guess towards the end of those -- of that initial ten years is when I started doing Raman.
Q. And did you characterize any pharmaceutical compounds using Raman in the first ten years of your career?
A. In those first ten years, no, we did not use Raman on pharmaceutical compounds.
Q. Have you --
THE VIDEOGRAPHER: I'm sorry to interrupt, Counsel, I have to apologize,

Page 22

Mr. McCreery, are you able to tilt your camera down just a little bit, please? If you can see yourself, we need you in the center of the video frame as best as possible. And then pan over just a little bit. Thank you.
BY MR. LOH:
Q. Have you synthesized any pharmaceutical compounds?
A. Well, I did actually make the radical ion derivative of chlorpromazine, which is the most -- the biggest psychotic of the '50s and '60s and '70s. That was an oxidation and crystallization of the -- of a material which then we characterized by a variety of techniques.
Actually, my first big paper in the Journal of American Chemical Society was about that synthesis and its properties and the material that I made. That I did personally.
Q. And when did you do that work on chlorpromazine?
A. I did that work on chlorpromazine, yes.
Q. When?

Page 23

A. When? Well, the JACS paper was published in 19 -- I've got to find it. My first -- yeah, yeah, that was published in 1978, so -- in JACS, which is the leading journal of the American Chemical Society. And as an aside, it's probably the paper that got me tenure. And so that was published in '78, so the synthesis would have been in '76, roughly, 1976.
Q. So that would have been before 1981 when you purchased your first Raman spectrometer?
A. That would be before I started doing Raman. All the Raman that I did was post-1981. And I went to the United Kingdom solely to learn how to do Raman from the fellow that invented surface-enhanced Raman.
Q. And you said that that work got you tenure. Was that at the Ohio State University?
A. Yeah, I got tenure approximately '79, '80. When you do a tenure evaluation, you look at the quality of the journals that they published in. And JACS is the best journal in chemistry, at the time, anyway, and so it was a major factor in the opinions of my colleagues and it ended up with me getting

Page 24

tenure. So I'd say that the body of work which involved -- which got me tenure involved this chlorpromazine experiments, but also some of the related spectroscopy that was not Raman spectroscopy, but involved UV-VIS and such.
Q. If we could turn to further in your CV, you have a publication numbered 134.
A. 134. Yes, I have it.
Q. This publication number 134 in your CV is from the Journal of Pharmaceutical Sciences. Do you see that?
A. Yes.
Q. And this is the publication you were referencing concerning Raman studies on materials from the FDA; is that correct?
A. Yes, yes. Spencer and Jefferson are both scientists at the FDA drug lab in St. Louis. And the question we were trying to answer, and answered, was whether Raman was useful for distinguishing pharmaceutical materials.
So we had 312 little brown vials of USP standards, and we ran spectra on all of those through the bottom of the vial, which is exceptional with spectroscopy, so with no

Page 25

sampling error and no sampling involved. We made a library out of those and then we tested the library to see how good you could distinguish drugs.

We also did a blind -- double-blind experiment where I told the student to pick out 25 of these 312 and don't -- and obscure the labels, give them to me, and then I ran them on a little Chromex spectrometer, which I helped develop with a startup company at the time. And I was able to identify all of them without a problem from the library.

So the point of that article was that Raman has got a lot of features in it which are very specific to the molecule. And if you -- that's why it's often called a fingerprint. And so Raman is very good at distinguishing material.

So it's possible today, it's very common today to take a handheld Raman spectrometer and point it at a white solid powder and determine what it is instantly. So that was the start of it.

And the other thing that we learned, which was -- which you could consider

Page 26

negative, is that some compounds also fluoresce and they -- fluorescence is much stronger than Raman, so you couldn't get a spectrum of, I think it was 8 percent of the 312 that we did. So it doesn't work on everything, but it does work reliably.

And there's a thing called a hit quality index that comes out of this library, the one that we used at the time, which tells you how good the match is, and that was very high.

So it clearly established that Raman was very good for distinguishing different white solids in that case inside brown vials without taking them out to sample them.

Q. So would you characterize Raman as a robust means of identifying pharmaceutical compounds?

A. I would, with the qualification that some pharmaceutical compounds or the materials that they're packed with can cause fluorescence, which is interference and masks the Raman. So I'd say that most things, yes.

In fact, I used an example in our discussion yesterday of a chemical weapons

Page 27

dump in Utah. And all the -- it's been there for 20 years and all the labels have fallen off, so they wanted to know what's in these nasty liquids. They can do that through the glass. So, yes, it's very good for that.

Q. How long did the work that's reported in this publication 134 of your CV take?

A. Sorry, could you repeat that?

Q. How long did the work that was reported in publication 134 of your CV take?

A. How long did it take?

Q. Yeah, how long did it take?

A. Oh, well, A.J. Horn, Angela Horn, did the spectra. To do 300 spectra, it takes a month maybe, maybe less than that. So it was several months of lab work and then some preparation of manuscripts, et cetera.

Q. How many spectra of each of those 300 or so materials did she take?

A. How many spectra?

Q. Yeah.

A. Of each one?

Q. Yeah.

A. Most of them were just -- were single spectra.

Page 28

Q. And who chose the 300 or so materials that were tested in this publication?

A. Did I what?

Q. Who chose the 300 or so --

A. Chose them?

Q. Yes.

A. Oh, well, the people at the FDA just sent us a couple of boxes and said here are 312 representative USP standards, have a go at it. They weren't chosen for Raman.

Q. And is this article that's listed at number 134 in your CV a peer-reviewed article?

A. Is that listed as what?

Q. A peer-reviewed article.

A. Peer reviewed, oh, yeah. Yeah. That's one of the leading journals in the field.

Q. Dr. McCreery, when did you last characterize any pharmaceutical compounds using Raman spectroscopy?

A. Well, we got into surface spectroscopy at that point, and so we didn't do very much with pharmaceuticals after that. I did encounter -- I worked with a couple of companies to make spectrometers, including the one used in that study. And they often

EXHIBIT C

A publication of the American Pharmaceutical Association and the American Chemical Society

JOURNAL OF Pharmaceutical Sciences

January 1998
Volume 87, Number 1

RESEARCH ARTICLES

Noninvasive Identification of Materials inside USP Vials with Raman Spectroscopy and a Raman Spectral Library

RICHARD L. MCCREERY*, ANGELA J. HORN, JOHN SPENCER, AND EVERETT JEFFERSON

Contribution from the *The Ohio State University, Department of Chemistry, 100 West 18th Avenue, Columbus, Ohio 43210, and FDA Division of Drug Analysis, 114 Market Street, St Louis, Missouri 63107.*

Received August 18, 1997. Accepted for publication October 20, 1997®.

Abstract ☐ A commercial dispersive Raman spectrometer operating at 785 nm with a CCD detector was used to acquire spectra of USP reference materials inside amber USP vials. The laser and collection beams were directed through the bottom of the vials, resulting in a 60% loss of signal. The Raman shift was calibrated with a 4-acetamidophenol standard, and spectral response was corrected with a luminescent standard. After these corrections, the Raman spectra obtained inside the USP vial and on open powders differed by less than 5%. A spectral library of 309 reference materials was constructed, with spectral acquisition times ranging from 1 to 60 s. Of these, 8% had significant fluorescent background but observable Raman features, while 3% showed only fluorescence. A blind test of 26 unknowns revealed the accuracy of the library search to be 88–96%, depending on search algorithm, and 100% if operator discretion was permitted. The tolerance of the library search to degraded signal-to-noise ratio, resolution, and Raman shift accuracy were tested, and the search was very robust. The results demonstrate that Raman spectroscopy provides a rapid, noninvasive technique for compound identification.

Introduction

Vibrational spectroscopy in the form of Fourier transform infrared (FTIR) absorption has long been used for materials identification. The combination of a rich spectral fingerprint and extensive spectral libraries results in a reliable and straightforward method for qualitative analysis of solid and liquid pharmaceuticals. However, FTIR generally requires sample preparation, and mid-infrared (MIR) light is strongly absorbed by most sample containers and fiber optics. So MIR spectroscopy is generally unsuitable for noninvasive observation of samples in glass or plastic containers and is difficult to interface with a remote location via fiber optics. The extension of MIR to noninvasive sampling would be very valuable for on-line or at-line process monitoring, but this prospect appears difficult except for special cases.

Near-infrared (NIR) absorption uses light in the 1−3 μm wavelength range and is compatible with fiber optics and glass containers. Remote and/or noninvasive sampling has been a major driving force for the development of NIR, particularly for quality control and process monitoring. Unfortunately, NIR absorption is based on combinations and overtones of mainly C−H stretches, and NIR spectra are not as information-rich as MIR spectra, which are based on fundamentals of a wider variety of molecular vibrations. Furthermore, NIR analyses often require multivariate calibration, which can be complicated by variations in water content or humidity. While NIR absorption is attractive from the standpoint of cost and sampling flexibility, the resulting spectra are not as specific nor as accurate as those from MIR spectrometers.

Although Raman spectroscopy has only recently been developed for analytical purposes, it has existed for more than half a century as a vibrational technique which provides spectral information similar to and often comple-

* Tel: (614) 292-2021. Fax: (614) 292-1685. E-mail: mccreery.2@osu.edu

® Abstract published in *Advance ACS Abstracts,* December 15, 1997.

S0022-3549(97)00330-4 CCC: $15.00
Published on Web 01/02/1998

mentary to MIR spectroscopy. Like MIR, Raman is based on fundamental vibrations and provides detailed spectral "fingerprints", but like NIR, Raman uses light which is compatible with fiber optics and many sample containers.[1,2] The selection rules for MIR and Raman are different, although in many cases the same molecular vibrations are observed. Raman requires a polarizability change while MIR or NIR requires a dipole moment change; hence, Raman is preferred for symmetric vibrations present in aromatic molecules, −S−S− bonds, C=C bonds, etc. Of value in pharmaceutical analysis is the relative strength of Raman scattering of aromatic drug substances compared to nonaromatic excipients, providing some selectivity for the drug. Raman spectra may be obtained noninvasively from solids and liquids inside vials or blister packs. This attractive combination of sampling and information content has not been exploited in the past for routine analysis because Raman used to be a complex and difficult technique, plagued by low sensitivity and fluorescence interference. These impediments have largely been eliminated by modern technology, notably NIR excitation (not to be confused with NIR absorption), CCD (charged coupled device) detectors, FT-Raman, and inexpensive computers.[2,3] Reliable, integrated Raman spectrometers are now available commercially[4] and are rapidly gaining acceptance as useful instruments for analytical chemistry. Applications of modern Raman spectroscopy to the analysis of pharmaceutical solids have been reviewed.[5]

Libraries of FT-IR spectra are extensive,[6,7] in both printed and electronic form, and new techniques continue to be developed. Several printed compendia of Raman spectra and characteristic frequencies are available,[7−10] and electronic versions are beginning to emerge. Specialized libraries for particular problems have been reported, including one for identification of urinary calculi[11] and for identifying spots on TLC plates.[12] A >5000 member FT-Raman library is available commercially in electronic form.[13]

The current work was undertaken to evaluate dispersive Raman spectroscopy with a 785 nm laser for identification of solid pharmaceuticals in amber vials. A 309-member spectral library was constructed from USP reference materials in USP vials, with the Raman light excited and collected through the vial bottom. Commercially available software (GRAMS/32, Galactic, Inc., Salem, New Hampshire) was used to search the test library and identify a group of blind "unknowns". The sensitivity of the search process to experimental parameters such as signal/noise, frequency error, and resolution was examined.

Experimental Section

The Raman spectrometer was a prototype version of the Chromex Raman 2000 with a 2050 sample chamber. Light from a Spectra Diode Labs SDL 8530 laser (785 nm) passed through a dielectric band-pass filter and then was focused through the bottom of standard USP amber vials. Backscattered light was collected by the same lens, passed through a Kaiser Notch Plus holographic laser rejection filter, and imaged onto the entrance slit of a Chromex 250 mm focal length imaging spectrograph. The detector was a EEV 15−11 (deep depletion) CCD in a Photometrics 270 controller. Unless noted otherwise, spectral conditions were as follows: laser power at sample, 50 mW on an approximately 100 μm diameter spot; 600 line/mm (1 μm optimized) grating; 50 μm slit width (resolution based on slit width = 3.4 cm^{-1} at 1500 cm^{-1}); spectral range 210−2060 cm^{-1}. Laser focus was adjusted for maximum signal from calcium ascorbate and then not readjusted for unknowns. Integration times varied from 0.1 to 60 s. Approximately 30 mW of laser light was transmitted to the sample through the USP vial, and there is a possibility of sample degradation for susceptible materials. None was observed in the current work, but prolonged integration times were not considered or required.

Raman shift was calibrated with naphthalene or acetamidophenol Raman shift standards (ASTM E 1848) and a quadratic fit of observed to standard values. Calibration with 10 peak frequencies for acetamidophenol between 329 and 1648 cm^{-1} yielded the most reproducible Raman shift values. Relative intensity was calibrated with a luminescent standard as described previously.[14] A sample of Kopp 2412 glass was placed inside an empty USP vial and its luminescent spectrum was obtained. The polynomial coefficients for the luminescence curve were those reported previously.[14] The reproducibility of these calibrations is discussed in the Results section.

A total of 309 USP standard reference materials were borrowed from the FDA drug analysis lab in St. Louis. GRAMS/32 Galactic, Inc. version 4.11 level II, and the "IR Search" add-on (version 3.14 initially, 3.18 finally) were used to construct and search the library. Library creation parameters were as follows: 1000 data points, 250−2000 cm^{-1}, 16 bit precision, X-axis in Raman shift, Y-axis in arbitrary units. Before spectra were added to the library, a two-point baseline chosen by Grams (with "baseline.ab") was subtracted from the spectrum after intensity calibration. The default points chosen by Grams were used, to avoid operator intervention and possible biasing. Of the 309 samples, 25 (8%) exhibited a relatively large fluorescent background, but still had observable Raman features, and 8 more (2.5%) showed only fluorescence. These samples were included in the library without discrimination. Before each day's acquisition of library spectra, instrument operation was verified by checking that frequency and relative intensity were within the limits described below. Library search algorithms are discussed in the results section.

Results

Dispersive/CCD spectrometers sample a particular Raman shift range, depending on grating selection, grating position, CCD size, etc. Figure 1 shows three spectra of calcium ascorbate, obtained with 300, 600, and 1200 line/mm gratings. Since there is a fixed number of CCD pixels along the wavelength axis (1024), there is an inherent tradeoff of resolution and spectral coverage. Thus the 1200 line grating yields high resolution (1.7 cm^{-1} for a 50 μm slit), but lower spectral coverage (~1000 cm^{-1}) than the 600 line grating (3.4 cm^{-1} and 2000 cm^{-1}). The library search software does not require that the spectral range of the unknown spectrum match that of the library, but it does require that all library spectra have the same spectral range. Because of the lack of Raman features between 1800 and 2800 cm^{-1} (for most samples), and because of the lower sensitivity of CCD's to the C−H stretch region (>2800 cm^{-1}), the 600 line grating was chosen to construct the library. This choice is a compromise of resolution and spectral coverage, at the cost of spectral information above 2000 cm^{-1}.

Figure 2 shows four spectra of pharmaceuticals obtained from solids inside USP vials. The great majority of the 309 USP samples exhibited spectra similar to the top two in Figure 2, with well-defined Raman features and integration times of 1−60 s. Ethylcellulose is an example of observable Raman features superimposed on a large fluorescence background. Approximately 8% of the spectra had a similar appearance. About 3% of the samples (8 out of 309) showed only fluorescence, such as dichlorophenylindolinone. Such samples are not amenable to Raman-based library searches, but even relatively small Raman features superimposed on fluorescence (such as for ethylcellulose) permit reliable qualitative identification. The fluorescence interference may be inherent in the molecule of interest, or it can be caused by fluorescent impurities. In general, fluorescence is decreased by operating at longer laser wavelengths, so a 785 nm system will exhibit fewer fluorescent samples than a 515 nm spectrometer but more than FT-Raman operating at 1064 nm.

The effect of sampling through an amber vial is illustrated in Figure 3 for acetamidophenol as an open

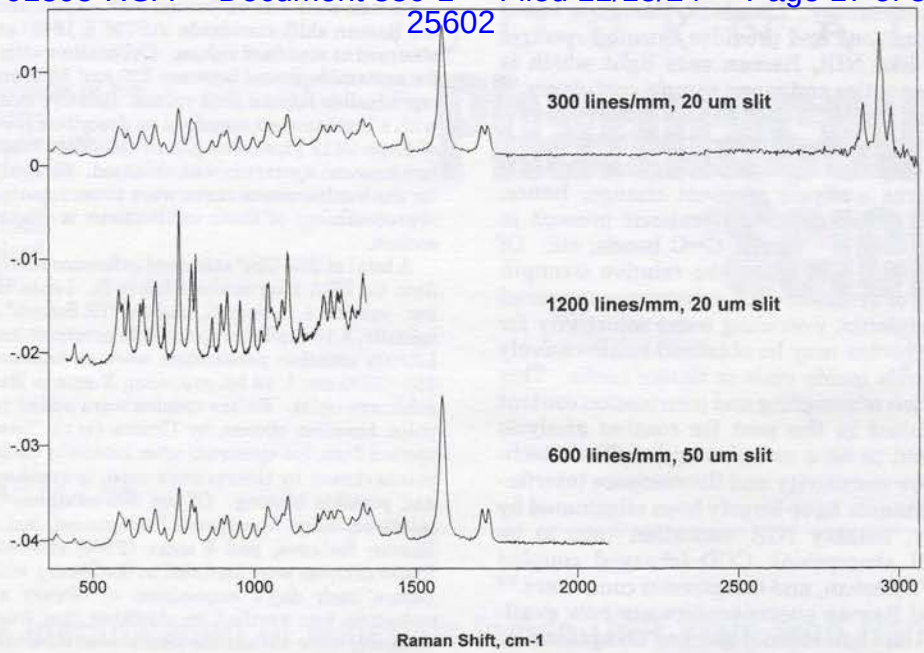

Figure 1—Raman spectra of calcium ascorbate acquired through the bottom of a standard USP vial. Three gratings were employed, and each spectrum is corrected for instrumental response; 52 mW (785 nm) light entering the vial and the integration time of 10 s in all cases.

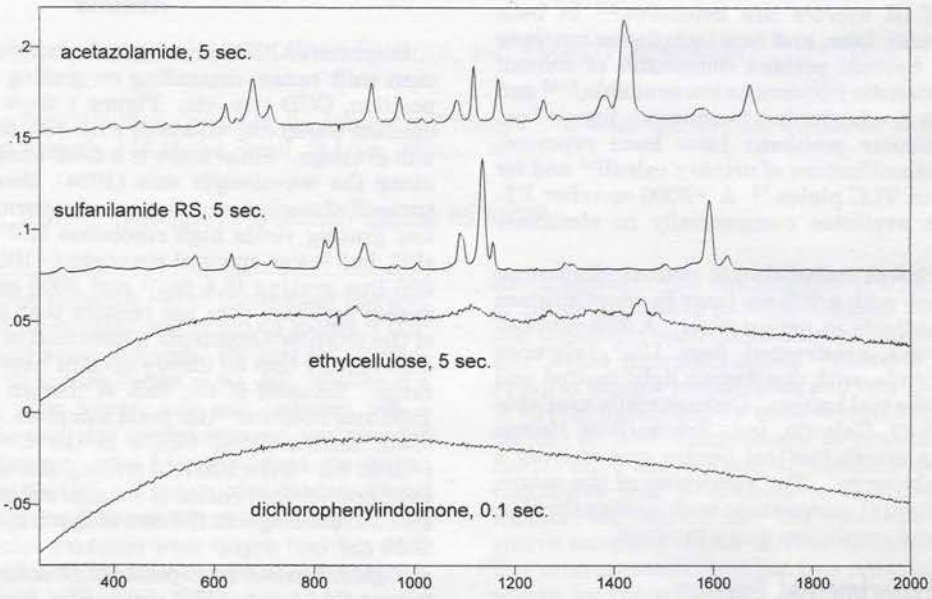

Figure 2—Raman spectra of USP reference materials inside USP vials: 600 line/mm grating, 50 μm slit width, 52 mW light entering vial. Compound names and integration times are as shown, and all spectra were corrected for instrument response.

powder and inside a USP vial. The spectrum of the open powder was corrected for relative intensity with an open piece of Kopp 2412 glass, while the vial spectrum was corrected with the Kopp glass inside the vial. For both sample and glass spectra, the focus was adjusted for maximum intensity, and the vial spectrum was subtracted as appropriate. The uncorrected spectra of both acetamidophenol and Kopp glass showed that the amber vial attenuated the signal to 41% of its value for the open sample, implying that the amber glass transmits about 64% each of the laser and Raman light. Since losses by vial transmission apply to both the sample and the Kopp glass intensity standard, they are corrected by the intensity calibration. The corrected spectra of acetamidophenol in Figure 3 differ in intensity by 5%. When the spectra are subtracted after adjusting for this difference, the maximum residual is 4%, and there is no trend across the Raman shift range observed. So both relative peak intensities and total Raman signal are corrected for vial transmission using the luminescent standard. Reproducibility of Raman frequencies and intensities was evaluated by obtaining spectra of calcium ascorbate in a USP vial over a several month period. The GRAMS peak-picking algorithm, which uses a center-of-gravity approach, was used to determine peak frequencies. For eleven Raman peak frequencies of calcium ascorbate, the standard deviations for six replicates on six different days ranged from 0.18 to 0.79 cm^{-1}, with all but one below 0.50 cm^{-1}. Twenty-three determinations of two calcium ascorbate frequencies over a 2 month period yielded standard deviation of 0.14 cm^{-1} for the 767.3 cm^{-1} band and 0.22 cm^{-1} for the 1582.7 cm^{-1} band. For fifteen replicates performed in one session but with random vial rotation between runs, three peaks showed standard deviations of 0.18–0.20 cm^{-1}. The raw intensities of Raman

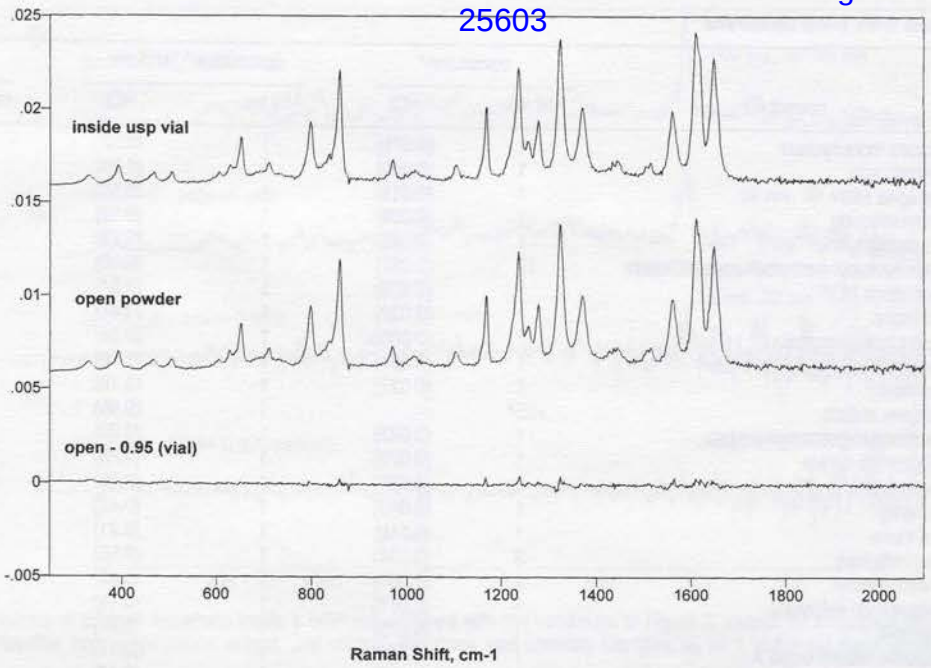

Figure 3—Raman spectra of 4-acetamidophenol obtained inside a USP vial and as an open powder, both corrected for instrument response. Conditions were the same as for Figure 2. The lower spectrum is the difference after multiplying the vial spectrum by 0.95. The same intensity scale was used in all cases.

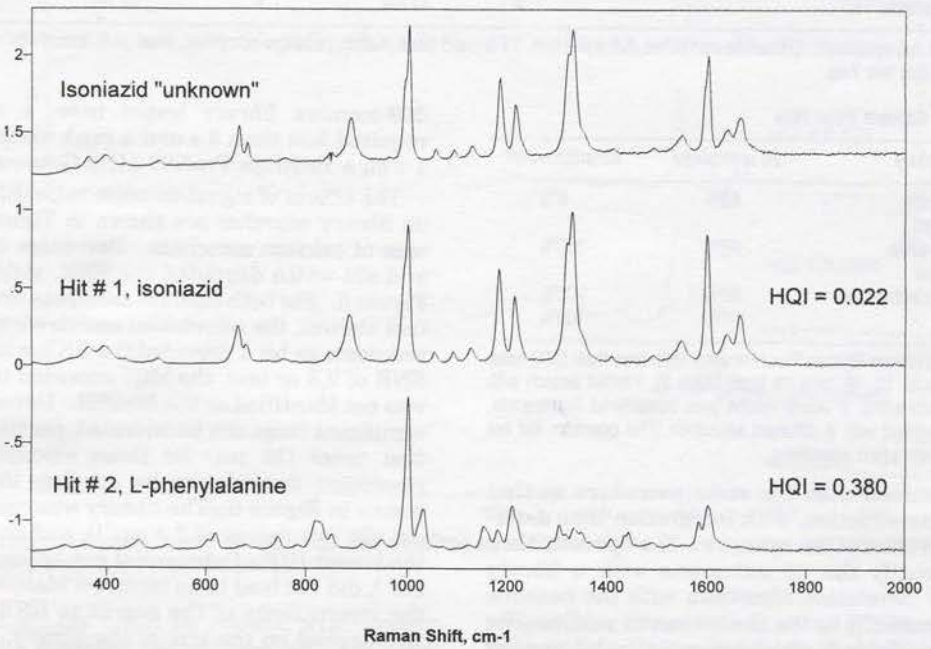

Figure 4—Example of a library search using the full spectrum/correlation search with baseline subtraction. "Hit 1" refers to the best match of the upper ("unknown") spectrum to 309 spectra in the library. HQI is the hit quality index, as discussed in the text.

bands varied approximately ±15% from day to day over a 2 month period, and about 5% for 15 runs on the same day with the vial rotated randomly between runs. The corrected peak intensity for the 1582 cm^{-1} calcium ascorbate band was 0.0116 ± 0.0009 (8%), and for the 767 cm^{-1} band, 0.00543 ± 0.00044 (8%) for 23 spectra over 2 months. The 767/1582 peak intensity ratio for these corrected spectra was 0.466 ± 0.011 (2.4%).

A typical library search result is shown in Figure 4, for a sample of isoniazid which was run separately from the library spectrum and whose identity was unknown to the operator. "Hit 1" is the first choice by the library search software from the 309-member USP library, "hit 2" is the second choice. Selection in this case was based on a "correlation" search, which searches for the library spectrum having the minimum difference for all Raman shifts, compared to the sample spectrum. Before this difference is calculated, both known and library spectra are normalized and mean-centered, which reduces differences in intensity and baseline offset. The correlation search is similar to, but generally more successful than the widely used "Euclidean distance" algorithm.[15] The "hit quality index" (HQI) ranges from zero for a perfect match to 1.0 for uncorrelated spectra. The low value of HQI for hit 1 in Figure 4 and the large increase in HQI for hit 2 adds confidence that hit 1 is correct.

Library accuracy was tested with a blind study of 26 unknowns chosen at random from the 309 USP standards.

Table 1—Search Results from Blind Unknowns

unknown	correct ID	correlation[a] hit no.	correlation[a] HQI	correlation[b] 1st deriv hit no.	correlation[b] 1st deriv HQI	peak match[c] hit no.	peak match[c] HQI
1	lactose monohydrate	1	(0.079)	1	(0.57)	1	(65.6)
2	benzoic acid	1	(0.045)	1	(0.24)	1	(99.2)
3	clonidine HCl	1	(0.018)	1	(0.11)	1	(85.5)
4	acetazolamide	1	(0.008)	1	(0.12)	1	(73.0)
5	guaifenesin	1	(0.042)	1	(0.23)	1	(50.8)
6	hydroxypropyl methylcellulose phthalate	17	(0.067)	1	(0.48)	1	(29.7)
7	molindone HCl[b]	1	(0.003)	5	(0.54)	4	(26.6)
8	naloxone	1	(0.032)	1	(0.44)	1	(58.6)
9	piperazine phosphate	1	(0.068)	1	(0.26)	1	(59.0)
10	beclomethasone dipropionate	1	(0.021)	1	(0.18)	1	(54.7)
11	isoniazid	1	(0.022)	1	(0.19)	1	(70.3)
12	atropine sulfate	>25[d]		1	(0.66)	1	(26.6)
13	medroxyprogesterone acetate	1	(0.023)	1	(0.20)	1	(65.2)
14	pilocarpine nitrate	1	(0.070)	1	(0.25)	1	(47.3)
15	mebrofenin	1	(0.037)	1	(0.25)	1	(51.09)
16	estradiol	1	(0.040)	1	(0.42)	1	(48.4)
17	amrinone	1	(0.016)	1	(0.21)	1	(70.7)
18	ethylcellulose	3	(0.034)	1	(0.55)	2	(26.1)
19	β-cyclodextrin	1	(0.083)	1	(0.42)	1	(55.9)
20	magnesium salicylate	1	(0.011)	1	(0.14)	1	(84.0)
21	lisinopril	1	(0.075)	1	(0.27)	1	(77.3)
22	glipizide related cmpd A	1	(0.088)	1	(0.14)	1	(77.3)
23	sulfanilamide RS	1	(0.015)	1	(0.13)	1	(75.0)
24	cisplatin	1	(0.038)	1	(0.26)	1	(44.1)
25	*p*-toluenesulfonamide	1	(0.16)	1	(0.15)	1	(31.3)
26	carteolol HCl	2	(0.23)	1	(0.14)	1	(53.9)

[a] Baseline corrected, full spectrum. [b] Baseline corrected, full spectrum. [c] Forward peak match, baseline corrected, level = 0, sensitivity = 10, standard. [d] Correct compound was not in first two hits.

Table 2—Percentage Correct First Hits

search procedure	26 unknowns	22 unknowns[a]
full spectrum correlation, baseline subtracted	88%	6%
correlation, first derivative, baseline subtracted	96%	100%
peak match, baseline subtracted	92%	100%
operator discretion[b]	100%	100%

[a] Unknowns with maximum Raman/Fluorescence ratio less than 0.30 were not included. (numbers 6, 12, 18, and 26 from Table 2). [b] Initial search with correlation/baseline subtracted. If visual match was considered inadequate, the spectra was researched with a different algorithm. The operator did not know the correct answer when searching.

Spectra were obtained with the same procedure as that used for library construction, with integration time determined at the discretion of the operator. The operator then attempted to identify the 26 unknowns with a library search using the correlation algorithm with the baseline subtracted automatically by the Grams search routine. The results are listed in Table 1, which indicates the hit number for the correct identification and the hit quality index. For both correlation searches, a HQI of 0 is perfect and 1 is uncorrelated, while for the peak match, a perfect match has a HQI of 100. Of the 26 unknowns, the library correctly identified the unknown as hit 1 for 22. All four misidentifications had high fluorescence, similar to the ethylcellulose spectrum in Figure 2. Before the list was unblinded, the author noted the poor visual match for these four (unknowns 6, 12, 18, and 26), and searched again with the "correlation, first derivative" algorithm, with and without baseline subtraction. Once the operator was satisfied with the visual match, all four were correctly identified as hit 1. Table 2 shows results for searches with different algorithms, with and without the four unknowns exhibiting high fluorescence. "Peak match" is a much faster search process which compares only peak positions and heights and is often used as an initial search. For the 309-member library tested here, a correlation search required less than 3 s and a peak match search less than 1 s on a Pentium Pro/200 MHz Gateway PC.

The effects of signal-to-noise ratio (SNR) and resolution on library searches are shown in Figures 5 and 6 for the case of calcium ascorbate. Decreases in integration time and slit width degraded the SNR, yielding the spectra of Figure 5. For both calcium ascorbate and acetamidophenol (not shown), the correlation search correctly identified the unknown as hit 1 provided the SNR was 3 or greater. For SNR of 2.5 or less, the HQI exceeded 0.6 and the sample was not identified as the first hit. However, it is clear that significant noise can be tolerated, permitting short integration times (10 ms) for these examples. The effect of resolution degradation by opening the entrance slit is shown in Figure 6. The library was constructed with a 50 μm slit (resolution of 3.4 cm^{-1}), and this slit width yields the lowest HQI. Substantial resolution degradation, to 34 cm^{-1}, did not lead to an incorrect identification. Of course, the insensitivity of the search to SNR and to resolution will depend on the size of the library, and the process is likely to be less forgiving with a larger library. Furthermore, a more sensitive spectrometer will yield a higher SNR for a given measurement time, and this higher sensitivity should improve the accuracy of the search.

In part because calibration procedures used in different labs have not been well-standardized, there is some variation in Raman shift values reported in the literature. These variations are generally 1–2 cm^{-1}, but can be as large as 5 cm^{-1}. The question arises of the sensitivity of library searches to such variations in observed peak frequencies, particularly since a given library may be used with different instrument types. To investigate this issue, the Raman shift axes of spectra of isoniazid and cisplatin were intentionally offset before searching. As shown in Table 3, the correlation search was fairly insensitive to Raman shift offsets up to 5 cm^{-1}. The peak match failed with smaller offsets, of 2 or 3 cm^{-1}. It is likely that Raman

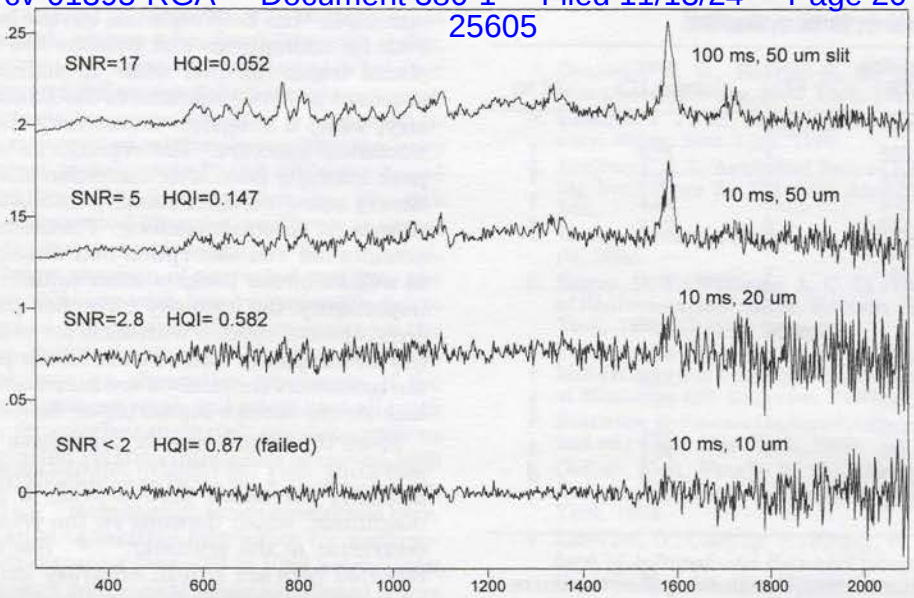

Figure 5—Corrected spectra of calcium ascorbate inside a USP vial obtained with the conditions of Figure 2, except for integration times and slit widths shown at the right. The HQI resulted from a correlation search, and calcium ascorbate was correctly identified as hit 1 in the top three spectra.

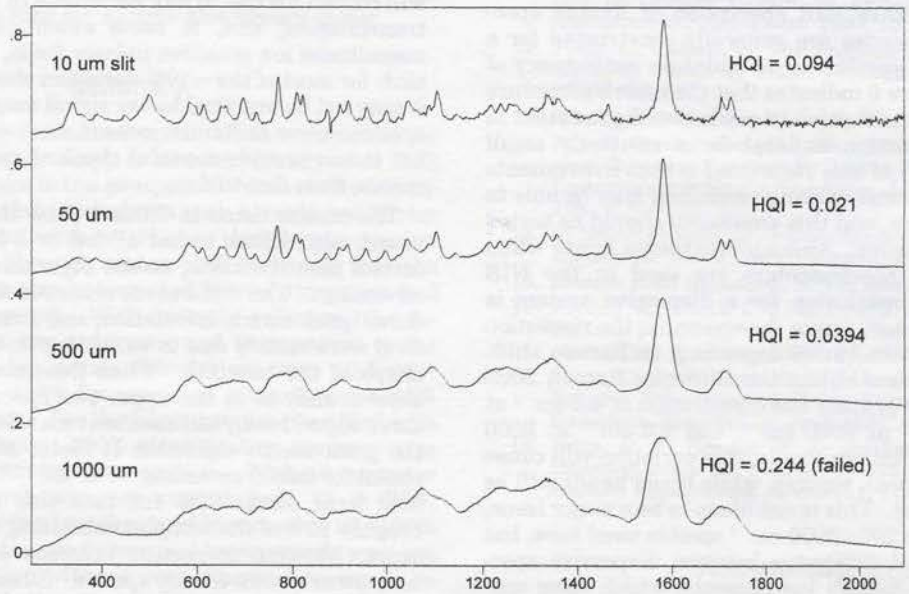

Figure 6—Corrected calcium ascorbate spectra (in USP vial) with conditions as in Figures 2 and 10 s integration time. Slit widths correspond to spectral resolutions (top to bottom) of <2, 3.4, 34, and 68 cm^{-1}.

shift accuracy of ± 1 cm^{-1} will be routine with modern instruments, and a standard deviation of <0.5 cm^{-1} was observed here for the 1582 cm^{-1} band of calcium ascorbate. So frequency inaccuracy should not be an issue if reasonable calibration procedures are followed.

Discussion

As noted in the results section, a dispersive multichannel spectrometer faces a tradeoff of spectral coverage and resolution, and the choice here was to use the 250–2000 cm^{-1} Raman shift range for the library. This range includes the "fingerprint" and "group frequency" regions and proved to be adequate for the unknowns and library size investigated. Since the C–H stretch region was not included, the question arises of how compound identification is affected by the absence of the C–H stretch frequencies. An advantage of FT-Raman is full spectral coverage regardless of resolution, so an FT library would be more sensitive to differences in C–H stretches. Since an analogous library with full spectral coverage is not currently available, the question of the cost of ignoring the C–H stretch region for the 309 compounds studied remains open.

Frequency accuracy is an important requirement for library searching and for spectral subtraction of spectral contributions from excipients or other materials. Fourier transform Raman instruments enjoy excellent frequency precision, but dispersive spectrometers do exhibit drift and jitter, sometimes as large as a few wavenumbers. The frequency precision observed for the current system of ± 0.50 cm or less was achieved by daily calibration with a Raman shift standard. Since the library searches were able to tolerate 2 cm^{-1} or more of frequency offset, the observed frequency precision should be more than adequate. In fact, ± 0.50 cm^{-1} is approximately equal to the standard deviation for a comparison of five FT-Raman and

Table 3—Effect of Frequency Shifts on Searches

frequency offset, cm^{-1}	correlation HQI	hit no.	peak match HQI	hit no.
		Isoniazid		
0	0.022	1	70.3	1
1	0.046	1	38.6	1
2	0.076	1	25.4	1
3	0.113	1	21.1	8
5	0.20	1		
7	0.29	1		
10	—	>10		
		Cisplatin		
0	0.027	1	44.1	1
1	0.054	1	31.6	1
2	0.078	1	21.1	2
3	0.106	1	29.7	1
4	0.138	1	20.7	3
5	0.173	1	20.3	8
10	0.348	1	—	

two dispersive spectrometers,[16] indicating that the current dispersive/CCD system has acceptable frequency accuracy.

Although variations in spectral resolution should not affect relative Raman band areas, they will affect relative peak heights, in either MIR absorption or Raman spectroscopy. FTIR libraries are generally constructed for a particular spectral resolution, to maintain consistency of peak heights. Figure 6 indicates that the search procedure used here is quite insensitive to resolution degradation in the unknown spectrum, at least for a relatively small library. A corollary of this statement is that instruments of different designs and varying resolution may be able to use the same library, and this possibility should be tested as library use increases. An additional issue arises when dispersive Raman spectrometers are used in the NIR region. Since the resolution for a dispersive system is constant in nanometers across the spectrum, the resolution in inverse centimeters varies depending on Raman shift. For example, a 50 μm slit in the Chromex Raman 2000 with a 600 line/mm grating has a resolution of 4.2 cm^{-1} at 200 cm^{-1}, 3.1 cm^{-1} at 2000 cm^{-1}, and 2.6 cm^{-1} at 3000 cm^{-1}. For narrow Raman bands, this variation will cause some distortion of peak heights, while broad bands will be only weakly affected. This is not likely to be a major issue, particularly for the 200–2000 cm^{-1} spectra used here, but it is a fundamental difference between dispersive spectrometers and FT-Raman instruments, which have constant resolution in inverse centimeters across the Raman spectrum.

Raman intensity calibration, both relative and absolute, is a much more complex issue than frequency calibration. MIR and NIR methods are based on a ratio of incident to transmitted light, while Raman generally involves only observation of scattered light. Since a MIR or NIR spectrometer measures the incident intensity, it corrects for instrumental response as a function of wavelength. Any variations in response with wavelength or time are compensated when the absorbance is calculated from incident and transmitted signals. Since Raman spectroscopy is generally a "single beam" technique without a reference intensity, Raman intensity is subject to rather large variations from detector response, focusing, alignment, laser power, transmission, etc. Such variations affect both the magnitude of the observed Raman signal and the relative intensities of peaks within a spectrum. Most of the Raman spectra in the literature are uncorrected for these possibly major variations in instrument response.

Response correction of dispersive Raman spectrometers with standard tungsten sources[17] and with luminescent standards[14] has been reported, but the latter was used here both for convenience and because the standard could be placed inside the USP vial. In addition, a luminescent standard precisely reproduces the Raman sampling geometry, while a tungsten source may differ in position or numerical aperture. The reproducibility of the 767/1582 peak intensity ratio after correction (2.4%) is important to library searches, since relative intensities are among the criteria for spectral matching. Furthermore, the correction accounts for vial absorption and would presumably work as well for blister packs or other containers. Perhaps most importantly, the intensity correction permits noninvasive acquisition of spectra with accurate relative peak intensities for samples in colored vials, blister packs, etc., provided the containers themselves are reasonably transparent and lack strong Raman scattering or fluorescence.

Since the library search normalizes the spectra before searching, only the relative intensities are important. The intensity correction does provide a meaningful signal magnitude, which depends on the cross section and concentration of the scatterer.[17–19] The signal magnitudes reported here are still in arbitrary units, since the Kopp glass emission was itself normalized before its polynomial was determined.[14] However, the signal magnitude does indicate scattering strength relative to the standard and will correct for day to day variations in laser power, optics transmission, and, to some extent, alignment. These magnitudes are sensitive to laser focus, which was responsible for most of the ~10% variation observed. At present, it may not be practical to use signal magnitude to compare spectrometers or Raman cross sections with high accuracy, but it can provide a useful check of spectrometer performance from day to day.

The results listed in Table 1 show that while the three search algorithms tested all led to a high percentage of correct identifications, no one algorithm exhibited a clear advantage. The differences observed for the three procedures (peak match, correlation, and correlation/first derivative) were mainly due to variations in the magnitude and shape of the baseline. When fluorescence was small or absent, such as in the upper two spectra of Figure 2, all three algorithms yield excellent matches. For such cases, the peak match algorithm is faster and is a reasonable choice for initial screening. For the USP standards examined here, about 90% fell into this category. For the roughly 10% of the samples exhibiting significant fluorescence, baseline correction becomes an issue, both for unknowns and for library spectra. Since the slowly varying baseline rarely contains any vibrational information, the safest approach is to use the correlation/first derivative algorithm. However, this approach is sensitive to noise and may fail for spectra containing spikes or discontinuities. The Grams software includes a linear baseline subtraction (srchbase.abh) based on the GIFTS algorithm, which results in a spectrum with all-positive points after subtracting a line whose slope and intercept are determined by the algorithm. The automatic two-point baseline correction used here is another Grams option, as are various procedures based on polynomial fits to the baseline or Fourier smoothing.

A major issue in any application of library searching is the transferability of a library to instruments of a different manufacturer or design. For a given laser wavelength, libraries of corrected spectra should be transferable, particularly if the resolution is kept constant. The intensity correlation compensates for instrument response and absorption by the sample container, so relative intensities should be reproducible for different instruments. Figure 6 shows that the search tolerates significant resolution changes, a fact which should improve transferability. If

the library is not corrected for intensity with a luminescent or tungsten standard, library transferability will suffer. The search approach used here is fairly tolerant of relative intensity variation and did successfully identify an uncorrected calcium ascorbate spectrum using a corrected library. However, uncorrected relative intensities can vary severely for different instruments,[14] and a library based on uncorrected spectra will be less transferable. The risk entailed in using uncorrected libraries is difficult to assess in a general manner but certainly should be kept in mind.

Even if the library consists of corrected spectra, the relative intensities will vary with laser wavelength due to resonance effects and the dependence of intensity on the fourth power of the Raman frequency (ν_r^4). When the laser wavelength is far from an absorption maximum of the sample, resonance effects are weak and intensities all track ν_r^4. For example, for colorless materials with absorptions in the UV, the corrected relative intensities observed with a 785 nm laser will be similar to those for a 1064 nm laser. For the 250−2000 cm^{-1} Raman shift range considered here, the maximum change in relative intensities for nonresonant samples when changing from 785 to 1064 nm is about 20%. This difference is not likely to cause significant errors for library searches conducted with 785 or 1064 nm spectrometers. Nevertheless, resonance or preresonance effects can be present, and care should be exercised when the laser wavelengths for sample and library differ.

Summary

As noted in the Introduction, the main motivation for adding Raman spectroscopy to more commonly used MIR and NIR techniques is the prospect of noninvasive identification of materials in containers such as vials and blister packs. The current work establishes that Raman spectra may be obtained through amber USP vials and that the relative intensities may be corrected for vial absorption and instrumental response. With suitable software, the required corrections are automatic and transparent to the operator. Day to day standard deviations were <0.5 cm^{-1} for Raman shift, <10% for corrected intensity, and <3% for relative intensity. For the blind samples identified with a 309-member library, 100% identification accuracy was achieved with operator intervention. Without operator intervention, search accuracy ranged from 88 to 96%, depending on search algorithm, and improved to 96−100% when samples with large fluorescent backgrounds were not included. Operation without user intervention would be important for production line applications, where the user may be unfamiliar with spectroscopy. For a large number of analyses where fluorescence can be avoided, an unattended library search can yield an accurate materials identification, while retaining the advantages of noninvasive operation, no sample preparation, and rapid analysis time.

References and Notes

1. Grasselli, J. G.; Bulkin, B. S., Eds. *Analytical Raman Spectroscopy*; Wiley: New York, 1991.
2. Laserna, J. J., Ed. *Modern Techniques in Raman Spectroscopy;* Wiley: New York, 1996.
3. McCreery, R. L. Analytical Raman Spectroscopy: an Emerging Technology for Practical Applications. *Am. Lab.* **1996**, 34x.
4. Henry, C. Raman Shifts Into High Gear. *Anal. Chem.* **1997**, *69*, 309A.
5. Bugay, D. E.; Williams, A. C. In *Physical Characterization of Pharmaceutical Solids*; Brittain, H. G., Ed.; Dekker: New York, 1995; Chapter 3.
6. For example: Chen, C. C.; Li, Y.; Brown, C. W. Searching a Mid-IR Spectral Library of Solids and Liquids with Spectra of Mixtures. *Vib. Spectrosc.* **1997**, *14*, 9.
7. Schrader, B. *Raman/Infrared Atlas of Organic Compounds*, 2nd ed.; VCH: New York, 1989.
8. Dollish, F. R.; Fately, W. G.; Bentley, F. F. *Characteristic Raman Frequencies of Organic Compounds;* Wiley: New York, 1974.
9. Lin-Vien, D.; Colthup, N.; Fately, W. G.; Grasseli, J. *Handbook of Infrared and Raman Characteristic Frequencies of Organic Molecules;* Academic Press: New York, 1991.
10. Nakamoto, K. *Infrared and Raman Spectra of Inorganic and Coordination Compounds,* 5 ed.; Wiley: New York, 1997.
11. Hong, T. D.; Phat, D.; Daudon, M.; Nguyen, Q. D. Identification of Urinary Calculi by Raman Laser Fiber Optics Spectrometer. *Clin. Chem.* **1992**, *38*, 292.
12. Petty, C.; Cahoon, N. The Analysis of Thin Layer Chromatography Plates by NIR Ft-Raman. *Spectrochim. Acta A* **1993**, *49A*, 645.
13. Nicolet Instruments, Madison, WI.
14. Ray, K. G.; McCreery, R. L. Simplified Calibration of Instrument Response Function for Raman Spectrometers Based on Luminescent Intensity Standards. *Appl. Spectrosc.* **1997**, *51*, 108.
15. *IR Search/Sadtler for Grams/386 Software Manual*, Galactic Industries: Salem, New Hampshire, 1995, pp 94−97.
16. *Raman Shift Standard*, ASTM standard E 1848, in press.
17. Fryling, M.; Frank, C. J.; McCreery, R. L. Intensity Calibration and Sensitivity Comparisons for CCD/Raman Spectrometers. *Appl. Spectrosc.* **1993**, *47*, 1965.
18. Petty, C. J.; Warnes, G. M.; Hendra, P. J.; Judkins, M. Relative Calibration of Single Beam Near Infrared Spectrometers. *Spectrochim. Acta* **1991**, *47A*, 1179.
19. Petty, C. J.; Hendra, P. J.; Jawhari, T. A Standardized Intensity Scale for Fourier Transform Raman Spectra of Liquids. *Spectrochim. Acta* **1991**, *47A*, 1189.

Acknowledgments

This work was supported by the National Science Foundation Division of Analytical and Surface Science and by an NSF STTR grant to Chromex and the Ohio State University. The authors thank Anthony Lombardo, for initial spectra obtained from USP samples, and Chromex, Inc., for technical assistance and equipment loans.

JS970330Q

EXHIBIT D

Raman Spectroscopy for Chemical Analysis

CHEMICAL ANALYSIS

A SERIES OF MONOGRAPHS OF ANALYTICAL CHEMISTRY AND ITS APPLICATIONS

Editor
J. D. WINEFORDNER

VOLUME 157

A JOHN WILEY & SONS, INC., PUBLICATION

New York / Chichester / Weinheim / Brisbane / Singapore / Toronto

Raman Spectroscopy for Chemical Analysis

RICHARD L. McCREERY

The Ohio State University
Columbus, Ohio

WILEY-INTERSCIENCE

A JOHN WILEY & SONS, INC., PUBLICATION

New York / Chichester / Weinheim / Brisbane / Singapore / Toronto

This book is printed on acid-free paper. ♾

Published simultaneously in Canada.

For ordering and customer service, call 1-800-CALL-WILEY.

Library of Congress Cataloging-in-Publication Data:

McCreery, Richard L.
Raman spectroscopy for chemical analysis / by Richard L. McCreery.
p. cm. — (Chemical analysis ; v. 157)
"A Wiley-interscience publication
Includes index
ISBN 0-471-25287-5 (alk. paper)
1. Raman spectroscopy. 2. Chemistry, Analytic. I. Title. II. Series.
QC454.R36.M33 2000
543'.08584 — dc21 99-086491

Printed in the United States of America.

10 9 8 7 6 5 4 3 2

CONTENTS

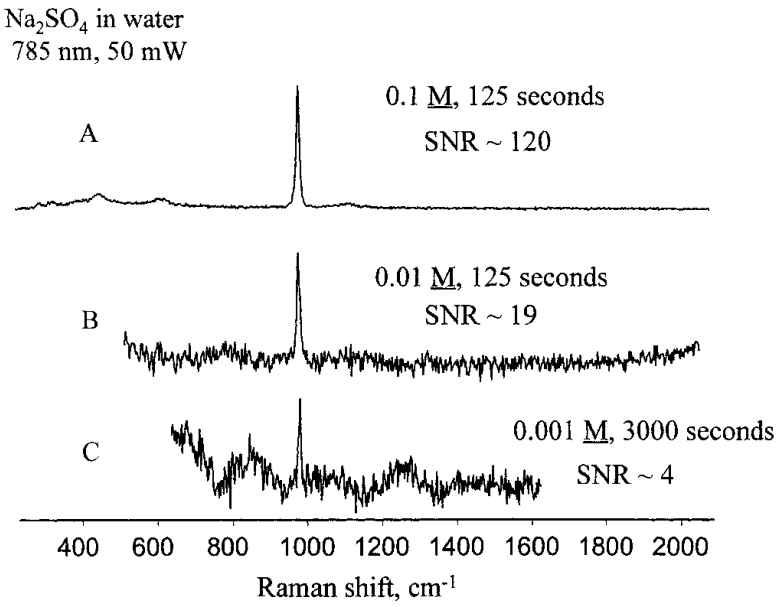

Figure 5.10. Spectra of Na_2SO_4 solutions, all after subtraction of water in cuvette background. Conditions as in Figure 5.9, except: (A) 0.1 M Na_2SO_4, average of five 25 sec integrations; (B) 0.01 M Na_2SO_4, average of five 25 sec integrations; (C) 0.001 M Na_2SO_4, average of sixty 50 sec integrations.

relatively long laser wavelength in this case (785 nm) yields a modest detection limit (for SNR ~3) for this system of just under 0.001 M.

5.5.4. White Solid with Weak Raman Scattering

White powders can present a challenge, since they generate a large elastic scattering signal. Several percent of the incident laser light may be scattered elastically into the spectrometer, representing a signal that is 10^4 to 10^8 times as strong as the Raman scattering. When the white solid is also a weak Raman scatterer, the sample becomes a severe test of both spectrometer sensitivity and laser light rejection. Powdered sucrose, lactose, dextrose, and the like are good examples of strong elastic scatterers with moderate Raman signals, and reasonable spectra should be obtainable with most spectrometers (e.g., see Fig. 5.16). Carbopol is a pharmaceutical excipient that is quite challenging, as it also has moderate fluorescence. Figure 5.11 shows spectra obtained with a 785 nm dispersive system and an FT-Raman system.

5.5.5. Fluorescent Samples

A discussed in Section 5.2, the choice of laser wavelength is often governed by background fluorescence, which generally decreases at longer wavelength. Rhodamine 6G is an example of a strongly fluorescent sample when observed

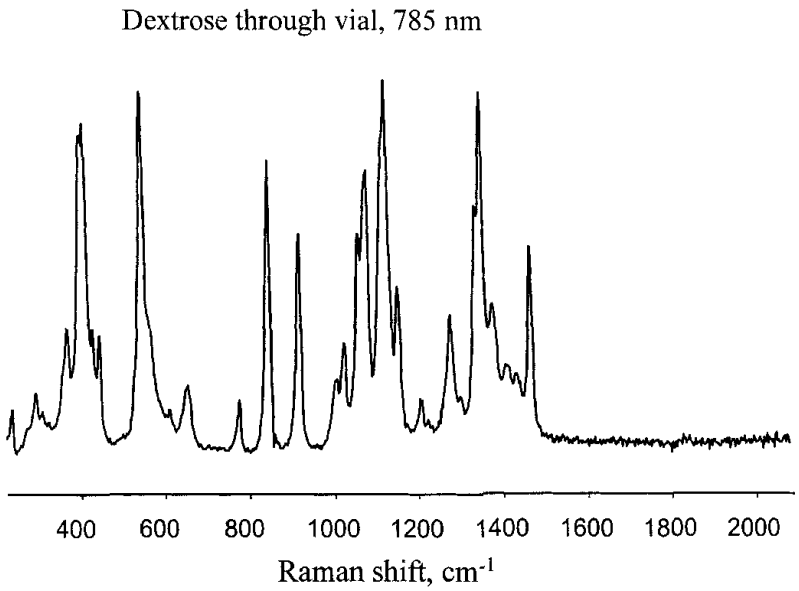

Figure 5.16. ACS reagent grade dextrose (glucose) solid inside USP amber vial. Conditions of Figure 5.9, average of five 10 sec integrations. Beam entered through bottom of USP vial, and vial spectrum was subtracted.

5.5.7. Through-Glass Sampling

The ability to obtain spectra of samples contained in glass or plastic vials without sample preparation is an attractive feature of Raman spectroscopy, since it permits noninvasive and nondestructive sampling. Not all spectrometer configurations can successfully observe samples in vials, due to optical geometry, working distance, or unsuitable laser wavelength. Of course, sample containers vary widely in thickness, shape, and material, but one example is shown in Figure 5.16. A USP (United States Pharmacopeia) amber vial is a standard container (with reproducible properties) used in the pharmaceutical industry, with a thickness of amber glass of about 3 mm (14). Figure 5.16 shows a spectrum obtained with 785 nm light directly through the bottom of the USP vial, with 180° geometry.

5.5.8. Response Uniformity

As noted in Section 5.4.2 and discussed in detail in Chapter 10, the relative peak heights observed in Raman spectra are strong functions of instrumental variables. These variations can be corrected, but it is useful to have a standard with known intensities in order to evaluate the instrument and the correction procedure. Figure 5.17 shows raw and response-corrected spectra of cyclohexane for 785 excitation. The relative peak areas for cyclohexane vary with

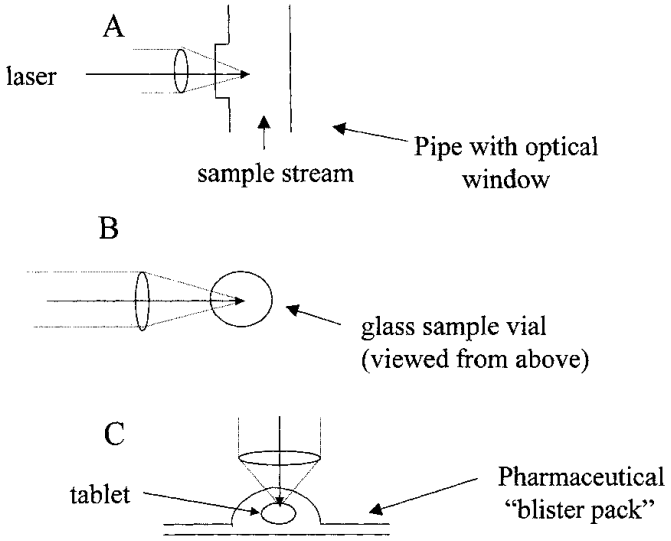

Figure 6.7. Noninvasive 180° sampling into a flowing stream (A), sample vial (B), or pharmaceutical blister pack (C). Optical window in case 6.7A is often made of sapphire to withstand possibly high pressure.

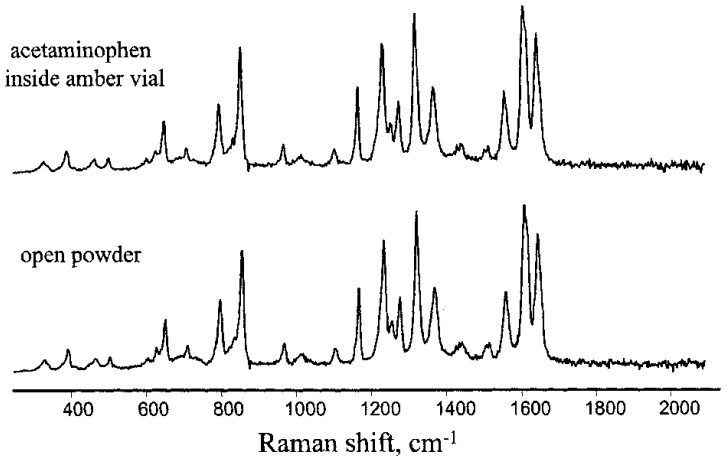

Figure 6.8. Spectra of acetamidophenol (active ingredient of Tylenol) obtained with geometry of Figure 6.7B. Spectra were response corrected as described in Chapter 10. Despite attenuation by amber vial, the corrected spectra differ by less than 5 per cent.

6.3.2. Sampling Volume for 180° Geometry

Chapter 3 and Eqs. (3.6) to (3.8) demonstrated that a Raman signal is proportional to a "geometric" factor K, which is related to sampling volume. For the case of 180° geometry shown in Figures 3.1 and 3.2, K is the incremental path length (dz) in the sample monitored by the spectrometer and illuminated by

Table 6.4. Reproducibility of Raman Signal for 180° Geometry[a]

Sample	Integration Time[b] (sec)	Relative Standard Deviation[c] (%)
1. Silicon wafer, motionless	10	0.42
2. Silicon wafer, remove and replace	10	0.78
3. CH_2Cl_2 in cuvette, motionless	0.5	0.63
4. CH_2Cl_2 in cuvette, motionless	2.5	0.31
5. CH_2Cl_2, remove and replace	2.5	0.82
6. Clear, solid polystyrene	2.5	0.78
7. Calcium ascorbate in amber vial	30	4.9
8. Heterogeneous tablet,[d] motionless	1.5	0.70
9. Tablet,[d] incremental lateral motion	1.5	12.6
10. Tablet,[d] remove and replace	1.5	13
11. Tablet, defocused, remove and replace	1.5	3.1
12. Tablet, line focus, remove and replace	1.5	6.0
13. Tablet, line focus, spinning, remove and replace sample	1.5	1.5

[a]Chromex Raman 2050, configuration of Figure 6.4D, $L_I = 75$ mm, $f/4$.
[b]For each run.
[c]From peak heights of 10 spectra.
[d]Acetaminophen, cellulose, magnesium stearate pressed tablet, heterogeneous on a roughly 50 μm scale.

Table 6.4 also illustrates a possible source of irreproducibility when dealing with solid samples. Mixtures of solids pressed into pellets are heterogeneous on a size scale comparable to the particles or microcrystallites of the solids involved. A common example is a pharmaceutical tablet, consisting of a physical mixture of drug and excipient (and possibly other components). As shown in Figure 6.14, the small laser focus (usually less than 50 μm) may preferentially sample one sample component or another, even if the focus is reproduced perfectly. Depending on the relative population of sample components under the beam, the apparent composition may vary with sample position. This effect is apparent for lines 8 to 12 of Table 6.4, which deal with a tablet of acetamidophenol formulated with magnesium stearate and microcrystalline cellulose. Although the reproducibility for a homogeneous solid was <1 per cent, the Raman signal for the tablet varied by 13 per cent when the tablet was removed and replaced. This variation was also observed for incremental lateral motion of the tablet, which did *not* affect the focus. If the focus was intentionally degraded so a larger region of the tablet was sampled, the run-to-run reproducibility improved from 11.3 to 3.1 per cent. Thus, the irreproducibility in

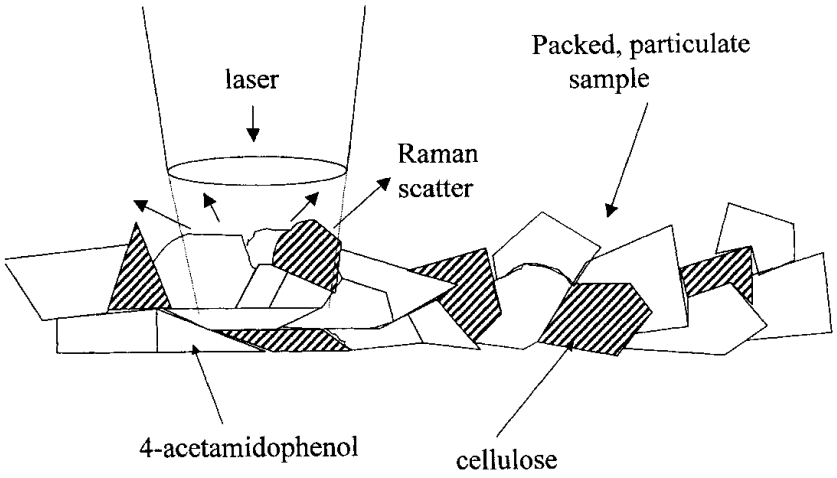

Figure 6.14. Schematic of laser focus on a heterogeneous sample consisting of acetamidophenol and cellulose pressed into a tablet. For repeated positioning of samples at the laser focus, the relative amounts of the two materials will vary.

this case was caused by a sampled volume that was small compared to sample heterogeneity. As described in Section 6.5, a line focus of the laser can cover more sample area without losing signal, thus averaging out much of the sample heterogeneity. The "line" focus of line 12, Table 6.4, samples an approximately 50 × 2000 μm area of the tablet and reduces the rsd for repeated replacement of the sample from 12 to 6 per cent. Further spatial averaging may be achieved by spinning the sample under the line focus, thus covering the much larger sample area shown in Figure 6.15. As noted in Table 6.4, sample spinning combined with a line focus reduces the rsd to about 1.5 per cent for repetitive replacement of a heterogeneous sample.

6.3.5. Summary of 180° Characteristics

The performance criteria noted in Section 6.2 can vary over wide ranges for the 180° geometry, mainly depending on the choice of collection lens focal length. A short collection lens yields higher sensitivity, but also shorter working distance, higher power density at the sample, and shorter depth of field. A longer collection focal length relaxes the requirement for accurate focusing (due to greater depth of field) but at the cost of sensitivity. In both cases, the 180° geometry is quite reproducible because the laser and collection axes are coincident. Overall, the 180° geometry is more versatile than the 90° geometry and generally easier to use. If one includes microscopes and fiber-optic problems as examples of the 180° geometry, it is certainly the most popular collection configuration in commercial spectrometers.

Raman Spectroscopy for Chemical Analysis. Richard L. McCreery

ISBN: 0-471-25287-5

CHAPTER

11

RAMAN MICROSCOPY AND IMAGING

11.1. OVERVIEW OF RAMAN MICROSCOPY

It was recognized quite early that the 180° sampling geometry provides a means to combine a Raman spectrometer with an optical microscope, thus permitting Raman analysis of very small regions of a sample (1). Raman microscopy has been used widely for analysis of very small samples or small heterogeneities in larger samples. For example, a small visible impurity in a pharmaceutical tablet might be identified after visual observation with a microscope, then a Raman spectrum may be acquired through the same microscope. Since Raman spectroscopy often involves visible light, and optical microscopes are very well developed, there is a natural match between the two techniques.

The simplest form of Raman microscopy is acquisition of a spectrum from a single point on the sample. Although the spot size is usually much smaller for microscopic sampling than for the conventional 180° arrangement discussed in Section 6.3, the two experiments are conceptually identical. The user has the option of obtaining spectra from several points on the sample, but only at one location at a time. The experiment is often called *microspectroscopy*, and collection of spectra from several points is often dubbed *point-to-point mapping*. The advent of two-dimensional detectors permits a variety of more efficient methods for Raman microscopy in which the instrument monitors more than one point on the sample. These methods are categorized broadly as *Raman imaging*, and the result is a sample image based on spectroscopic information (2). For example, the image may be derived from light having a particular Raman shift, so that the spatial distribution of a particular component may be observed. Alternatively, it is possible with some instruments to choose any point on the stored spectroscopic image and then display its Raman spectrum. A third possibility is *profiling*, where the variation of intensity of a particular Raman feature is observed along a straight line on the sample.

Considered in a general context, these methods amount to different ways to acquire or display results from a data set of intensity as a function of four independent variables: x, y, z (depth), and Raman shift. A complete spectroscopic description of the sample is a hypercube of Raman intensity as a function of Raman shift and three spatial axes. Some authors refer to experiments

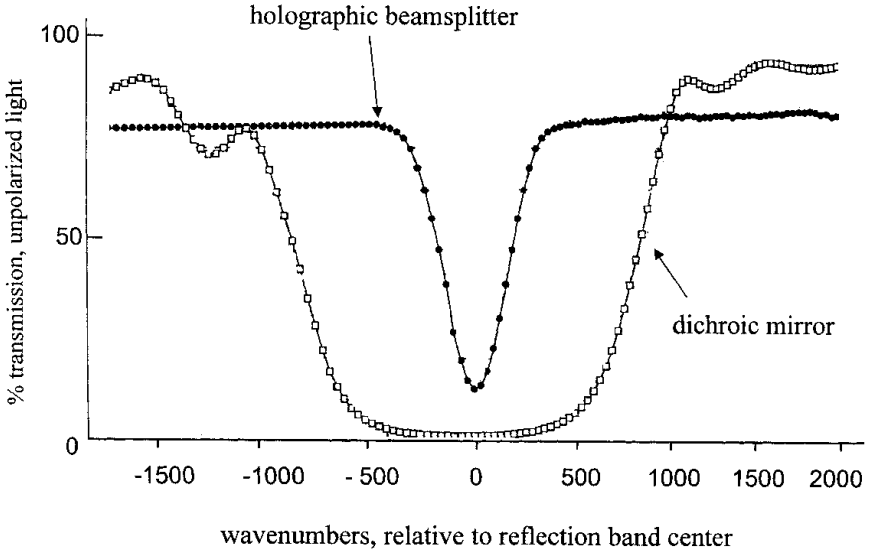

Figure 11.5. Transmission curves for dichroic mirror (squares) and holographic beamsplitter (dots). (Adapted from Kaiser product literature and described in Reference 4.)

An alternative to the smart beamsplitter exploits the high reflectivity of a holographic notch filter (Section 8.2.5.2) at the laser wavelength. When positioned as shown in Figure 11.6, a notch filter serves to insert the laser beam into the collection axis. Since the filter is at a near-normal angle to the collection axis, it transmits a high fraction of the Raman-shifted light into the spectrometer. In addition, the filter rejects elastically scattered light from the sample. So the notch filter is acting as both an efficient "beamsplitter" to combine the excitation and collection axes and as a notch filter to reduce stray light in the spectrograph. As with a dichroic mirror, the notch filter must be matched to the laser wavelength, taking into account the angle of the filter relative to the collection and laser axes.

An example of single-point Raman microspectroscopy is shown in Figure 11.7, in this case with a broadband beamsplitter. The sample is a pharmaceutical tablet pressed from a mixture of powdered acetamidophenol (active) and microcrystalline cellulose (excipient). The particle size is in the range of 10 to 50 μm, and the distribution of active and excipient is random. A conventional spectrometer with a spot size of ~100 μm yields a spectrum containing Raman features from both components, since it is spatially averaging over the <50 μm heterogeneities. The video micrograph shown in Figure 11.7 (often called a "bright-field" image) shows few features, as the two components are visually indistinguishable in this case. A typical macro spectrum, which sampled a 50 × 50 μm region of the tablet surface,

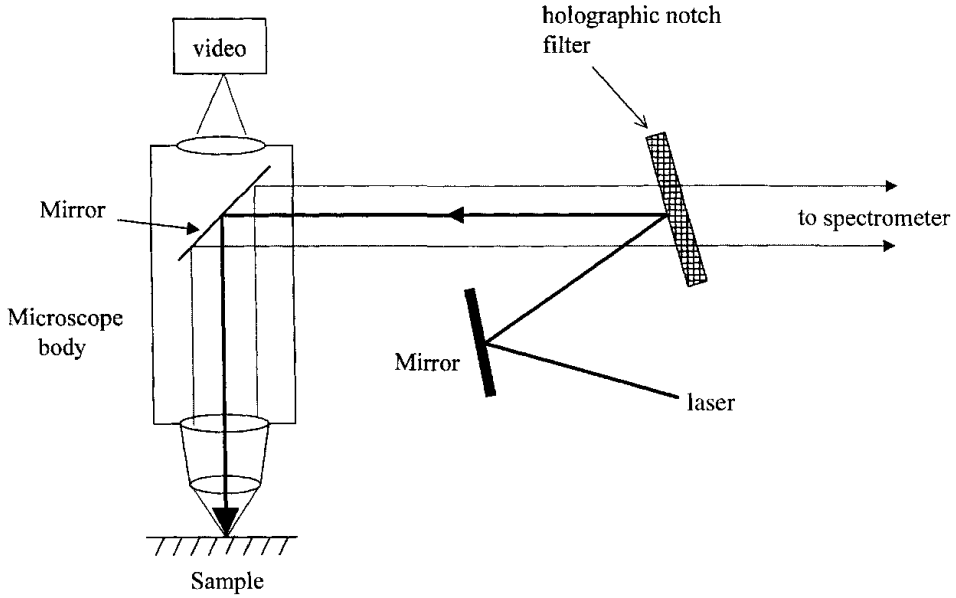

Figure 11.6. Schematic of holographic notch filter used to inject laser beam into the collection axis of a microscope (similar to an arrangement in a Renishew Raman microscope system).

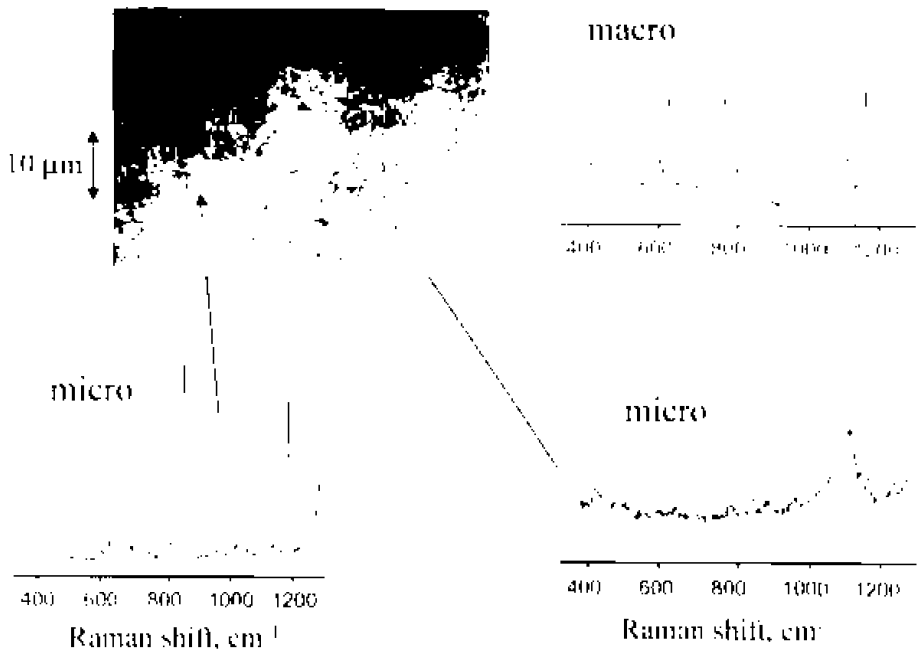

Figure 11.7. Single-point Raman microspectroscopy of a pressed tablet containing acetaminophenol and microcrystalline cellulose. The macro was obtained with an ~100 μm-diameter sampling area, and the micro spectra were obtained at the locations indicated.

shows features from both components of the mixture. Microprobe spectra of two locations on the tablet show distinct spectra for each component, since the spot size in this case is <10 μm. Notice that the "excipient" peak in the region of 1100 cm^{-1} is absent from the "active" spectrum, indicating nearly complete spatial segregation of the two compounds. Some additional examples of single-point Raman microspectroscopy are listed in Table 11.3. A specialized but impressive application is Raman microspectroscopy of single microdroplets with picoliter volumes that were laser trapped in an immiscible liquid (5). The microprobe provided a three-dimensional distribution of the Raman scatterer within the microdroplet with a spatial resolution in terms of solution volume of a few femtoliters.

A rudimentary type of Raman imaging is the line profile, consisting of a series of single-point spectra acquired along a line selected by the user. The total acquisition time equals the number of sample positions observed times the single-point acquisition time, plus any overhead associated with sample motion. Several commercial instruments automate the process with a computer-controlled microscope stage that positions the sample under the laser spot according to a video image. A line profile is shown in Figure 11.8, constructed of 31 spectra along a 90 μm line on an integrated circuit. All

Table 11.3. Examples of Raman Microscopy Applications

Configuration	Sample	Reference
Single-point sampling	Poly(ethylene terephthalate)	6
Single-point sampling of microdroplet	Toluene in water	5
Single point, confocal	Multilayer polymer film	7
Single point, confocal	Poly(ethylene terephthalate)	8
Single point	Borate minerals (caforsite)	9
Global and line imaging	Polystyrene/polyacrylate composite	10
Global imaging	Gallium arsenide semiconductor dots	11
Single point	Human dentin and resin composite	12
Line imaging		13
Line imaging	Polyvinyl chloride	14
Hadamard imaging	Benzoic acid	15
Mechanical line scan	TiO_2, zirconia	16
Single point	Carbon fibers	17
x-y image reconstruction from line scan	Glassy carbon and graphite surfaces	18
Hadamard imaging	Graphite surfaces	19
Global imaging	Human lymphocytes	20
Line imaging	CuSCN on platinum electrodes	21
Single point	Microorganisms	26

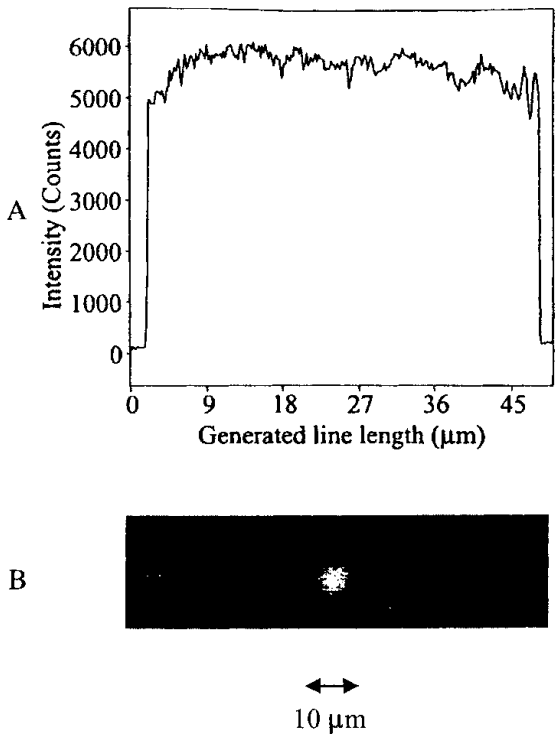

Figure 11.22. Illustration of the use of a Powell lens to flatten the intensity profile of a Gaussian laser beam. A is the observed laser intensity along a line focus at the sample, and B is a Raman image of two 6.7 μm diameter polystyrene spheres reconstructed from a collection of line images. (Adapted from Reference 23.)

In this case, a particularly sensitive spectrometer and an intensified CCD were used, so the images were obtained quite rapidly (8 sec to 2 min).

The mechanical line scanning technique described in Section 11.3.2 has also been extended to two-dimensional Raman imaging by the addition of a computer-controlled translation stage. The result is shown in Figure 11.23 for the same pressed pharmaceutical tablet used to illustrate microspectroscopy in Figure 11.7. In this case, the laser spot was mechanically scanned along a 60 μm line, and the corresponding image on the CCD was binned into 28 spatial elements. The line was monitored for a total of 180 sec, to produce 28 spectra, each containing 500 intensities as functions of Raman shift. The translation stage was incremented 28 times, and the 180 sec acquisition was repeated after each step. The result was a hypercube of intensity vs. x, y, and $\Delta\bar{\nu}$, with 28 × 28 spatial elements and 500 Raman shifts. So the total data set contained 392,000 intensity values, which could be accessed and manipulated after the experiment was over. Figure 11.23A shows the intensity of the 839 to 875 cm^{-1} region, which includes the 858 cm^{-1} band of the active ingredient, 4-acetamidophenol. The false color scale represents the most intense Raman

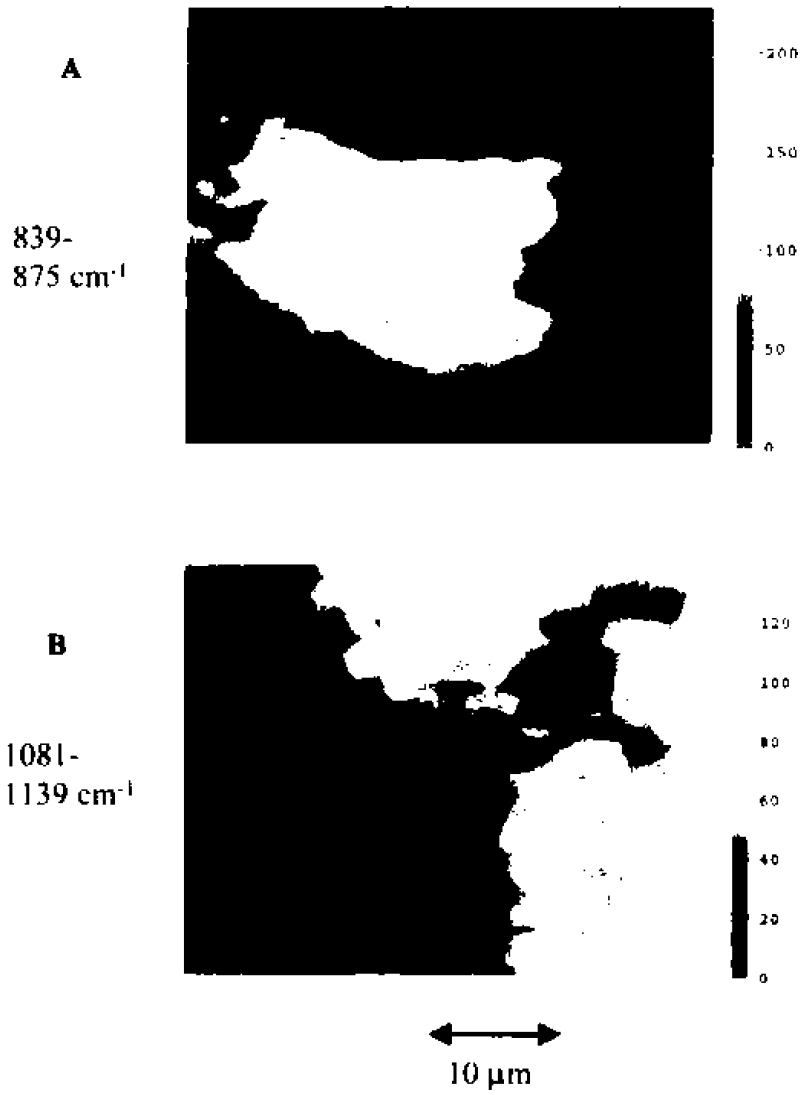

Figure 11.23. Raman images of a pharmaceutical tablet reconstructed from 28 line images obtained with mechanical line scanning in a Dilor "XY" spectrometer. Both images are of the same area on the tablet, but image A is derived from an acetamidophenol band, while image B is from an excipient band. False color intensity scale is shown to the right of both images. Individual spectra are shown in Figure 11.7. (See color plates.)

scattering as white and yellow and the weakest as black. It is clear from Figure 11.23A that the active ingredient is localized in a ~30 µm particle. The 1081 to 1139 cm^{-1} shift region contains a band due primarily to the excipient (Avicel), whose spatial distribution complements that of acetamidophenol. Two alternative representations of the data of Figure 11.23A are shown in Figure 11.24. The 839 to 875 cm^{-1} image in Figure 11.23A is

actually a spatially smoothed version of the raw 28 × 28 matrix shown in Figure 11.24A. The smoothing process is mathematically objective but cannot generate any new information. Figure 11.24B is a histogram of intensity vs. x and y, with intensity indicated by both height and color.

Both optical and mechanical line scans generate large data sets when used to construct a two-dimensional Raman image, but computer power and storage is inexpensive in the post-PC world. An advantage of such large data sets is the retention of complete spectra for each spatial element, with often high spectral

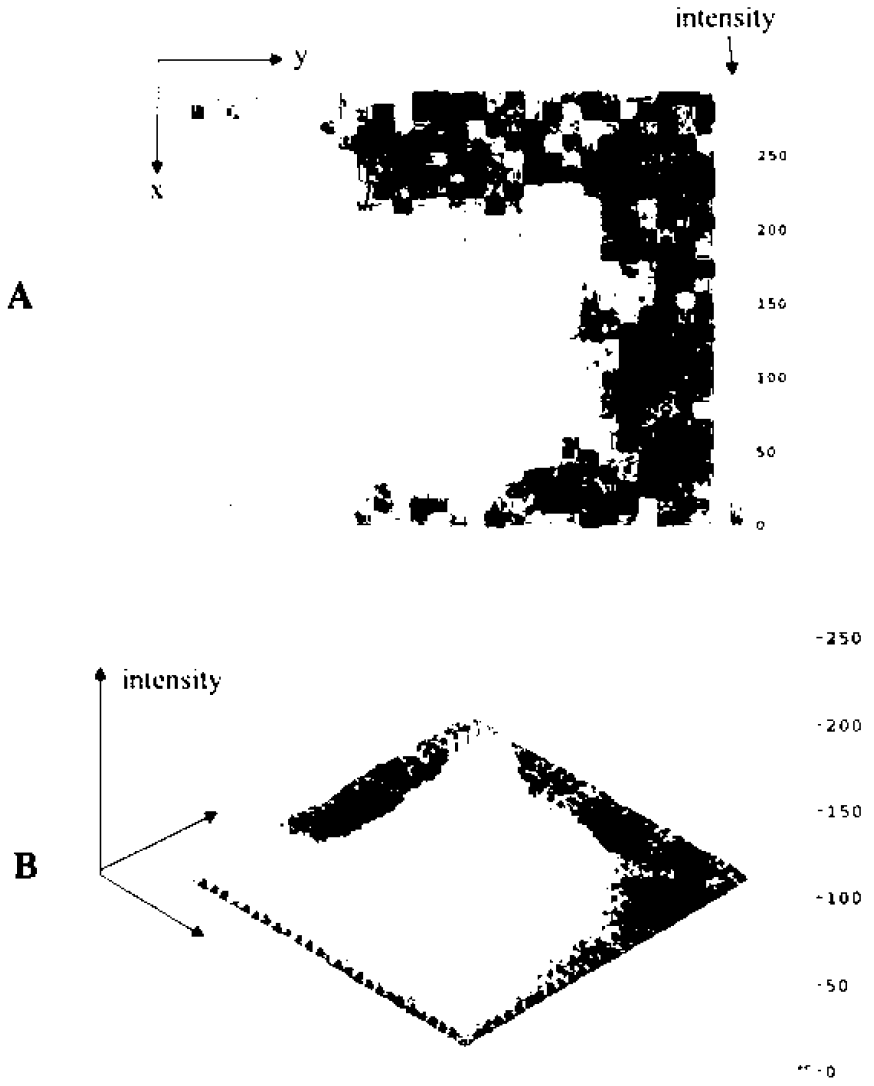

Figure 11.24. Alternative representations of the data in Figure 11.23A. Image A is the raw 28 × 28 spatial grid, with white representing the most intense 858 cm^{-1} band. Image B is an axonometric plot showing intensity as both a height above the x-y plane and as a false color scale, shown on the right. (See color plates.)

resolution. Data analysis techniques based on chemometrics and factor analysis may be applied to such data sets to provide greater chemical selectivity. A simple example is baseline subtraction in which a broad or sloping baseline is subtracted from each spectrum in each spatial element, leaving only Raman scattering. Fitting and subtracting baselines is more difficult with the limited spectral data from global imaging. Factor analysis is a general term that refers to the process of decomposing a series of spectra into components that describe variations among the spectra. In principle, every spectrum in an image may be described as a linear combination of a relatively small number of "factors," and each factor is often associated with a chemical component in the sample. The hyperspectral Raman data set is amenable to factor analysis, so that the spatial distribution of chemical components may be determined. Instead of observing the distribution of a particular Raman band (as in Fig. 11.23), the distribution of an entire *spectrum* is determined. The Raman image is more specific for a particular component when based on factor analysis, resulting in greater ability to localize particular chemical species.

The image of Figure 11.22B is based on the polystyrene "factor" and is obviously limited spatially to the polystyrene sphere itself. Factor analysis has the added benefit of automatic background correction, since the background is often due to a different sample component than the factor of interest. The ability of factor analysis to discriminate among similar chemical components is illustrated in Figures 11.25 and 11.26. A section of human biopsy tissue was mounted in paraffin for conventional analysis by a pathologist. The tissue slice contained paraffin plus several structurally similar biological lipids, all of which were distributed nonuniformly in the tissue section. The bright-field micrograph of Figure 11.25 shows both fibrous tissue and a region suspected of being a prostate tumor. Figure 11.25 also shows three single-point spectra obtained at different regions on the sample, as indicated. Since paraffin and the two naturally occurring lipids have long aliphatic chains, their spectra in the spectral region shown are similar but not identical. The software was instructed to determine the contribution of each of these three spectra to the spectrum observed at each spatial coordinate in the entire image. Figure 11.26 shows an overlay of the Raman analysis on the video image. Each color corresponds to the contribution from each of the three components, based on the entire spectrum. Although the spectra are similar to the eye, their spatial distributions based on factor analysis are clearly distinct. Assignment of each of the 28×28 spatial points to a particular lipid component by eye would have been at least tedious and probably inaccurate as well.

11.4.3.2 Hadamard Image Reconstruction

Hadamard transform spectroscopy existed long before Raman imaging, as a form of multiplex spectroscopy. A Hadamard mask is an array of clear and

length. Figure 12.14C is a spectrum of the same sample obtained with the DLT probe head of Figure 12.18, and 17 m cable length. The contribution of silica is negligible, even with the long fiber-optic length. The beamsplitter in Figure 12.18 is often a weak point in the design, due both to low efficiency and to contributions to the background. A simple 50 per cent reflective mirror will sacrifice 50 per cent of the laser light and 50 per cent of the Raman light, thus decreasing the possible signal by 75 per cent. This loss contributes to the significantly weaker signal apparent in Figure 12.14C compared to 12.14B. A dichroic mirror reduces this loss somewhat but must be changed for different laser wavelengths. Both types of mirrors generate inelastically scattered light, and their optical materials must be selected carefully to have low background. Overall, the simple design of Figure 12.18 provides reasonable performance at relatively low cost and has many of the attractions of more expensive probe heads based on holographic optics.

A more efficient design from Chromex, Inc. shown in Figure 12.19 uses a periscope arrangement to inject the laser beam into the collection beam axis. The turning mirror in the collection path is small, and represents a fairly small fraction of the collection lens area (~10 per cent). This injection loss is much smaller than that of a 50/50 beamsplitter, leading to higher overall probe efficiency. In addition, the fiber bundle used for collection may be reconfigured at the spectrometer to match the entrance slit, thus increasing the $A\Omega$ product. As with the design of Figure 12.18, the filters are less expensive than holographic optical elements and the probe design is quite versatile in terms of working distance and laser wavelength.

A spectrum of 4-acetamidophenol obtained with the Chromex probe head of Figure 12.19 is shown in Figure 12.20. The signal magnitude is comparable

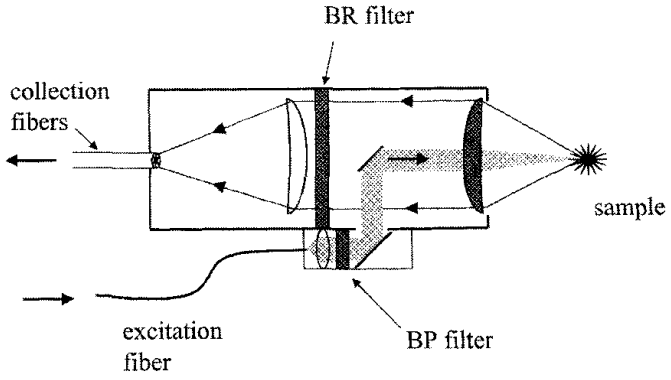

Figure 12.19. Schematic of the Chromex distally filtered fiber-optic probe, which uses a periscope arrangement to inject the laser beam into the collection axis (24). The collection fibers are arranged as a circular bundle in the probe, and a line at the spectrometer, matched to the entrance slit.

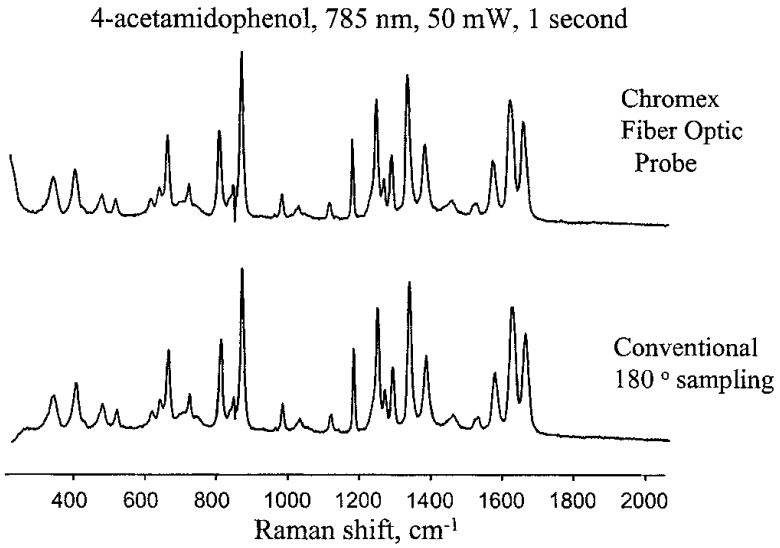

Figure 12.20. Spectra of acetamidophenol obtained with the fiber-optic probe of Figure 12.19 (upper spectrum) and with conventional 180° sampling (similar to that of Fig. 6.5D). In both cases, 50 mW of 785 nm laser power impinged on the sample, and other acquisition conditions were identical.

to that obtained with conventional 180° sampling, for the same integration time and laser power at the sample. A detailed study investigating quantitative analysis of intact pharmaceutical capsules using this probe has appeared (24), and the Raman results were of comparable accuracy to those from diffuse reflectance infrared spectroscopy. A significant advantage of the Raman approach was the lack of sample preparation and rapid, nondestructive data acquisition. Spectra of the active drug (bucindolol) at three different concentrations in an excipient are shown in Figure 12.21.

The high optical density of holographic rejection filters for laser light described in Section 8.2.5.2 is accompanied by a high reflection efficiency for the same laser light. So a holographic rejection filter may also be used as a very efficient mirror that selectively reflects a narrow band of wavelengths and transmits all others. This property of holographic filters is exploited in the Dilor "Superhead" design shown in Figure 12.22 (25). The excitation and collection fibers enter the probe head parallel but not coaxial, and the laser light is filtered to remove silica background. A holographic filter serves to combine the laser and collection axes, as well as reject much of the elastic scatter returning from the sample. An additional notch filter precedes focusing onto the collection fiber. As with the DLT and Chromex designs, the working distance may be varied easily by changing the objective lens.

A further refinement in head design improves the laser filtering by adding an additional holographic element. The Kaiser Mark II head shown in

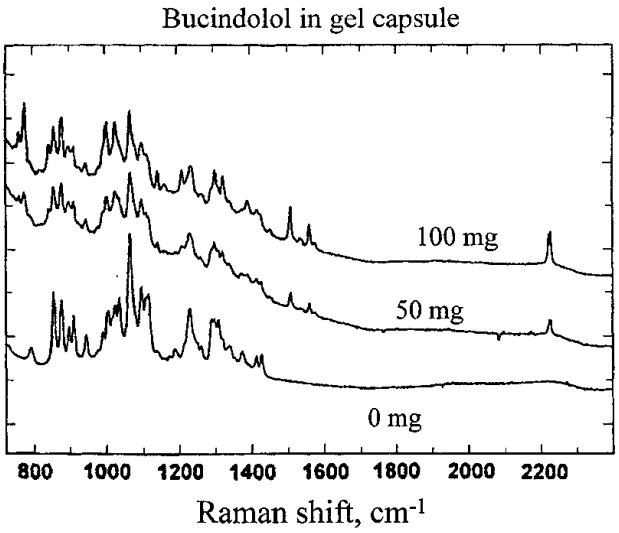

Figure 12.21. Raman spectra of bucindolol capsules with the Chromex probe and Raman 2000 spectrometer. The active drug had three different concentrations (0, 50, and 100 mg) in an excipient similar to lactose. The bands at ~2200 and 1400 to 1500 cm^{-1} are due to bucindolol, as are other less obvious bands overlapping the excipient features. The spectra were obtained on intact capsules, with the beam transmitted through the thin (and weakly scattering) gel capsule material. The 50 and 100 mg spectra are offset for clarity. (Adapted from Reference 24 with permission.)

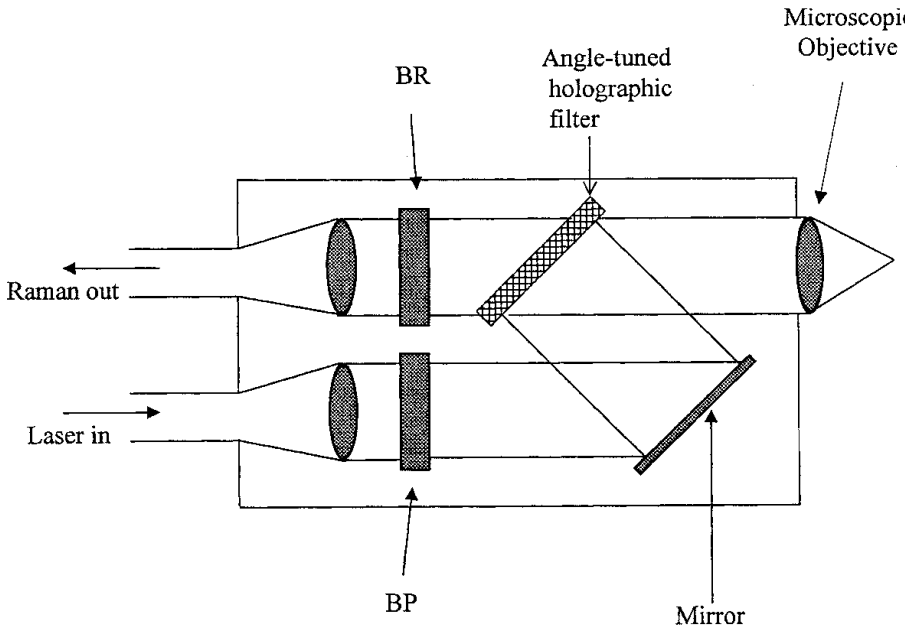

Figure 12.22. Schematic of Dilor "Superhead" fiber-optic probe head. The objective lens may be replaced to permit different working distances and focal spot diameters.

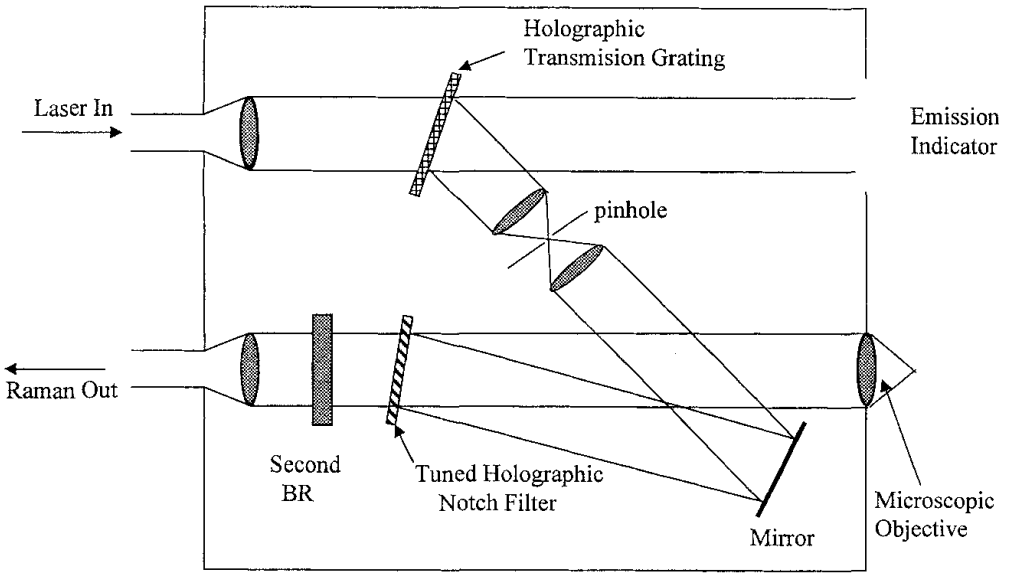

Figure 12.23. Schematic of Kaiser Mark II fiber-optic probe head. A holographic diffraction grating and pinhole act to remove silica scattering from the laser light and improve beam quality by spatial filtering. (Adapted from Reference 1 with permission.)

Ribonucleotides in 50 μm capillary, 532 nm, 2 W, 1 second

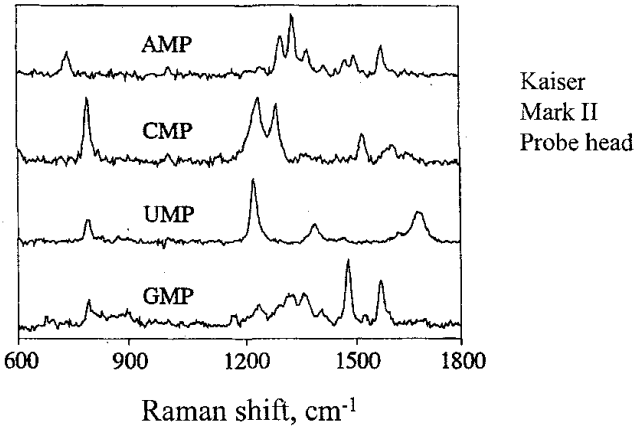

Figure 12.24. Spectra of dilute solutions of ribonucleosides obtained with the Kaiser Mark II probe and Kaiser spectrograph. Solutions were in a 50 μm capillary in which they had been concentrated by isotachophoresis. (Adapted from Reference 27.)

Figure 12.23 combines the holographic bandpass filter described in Chapter 7 (and Fig. 7.11) with an already efficient probe head (26). The holographic BP filter transmits a greater fraction of the laser light than a dielectric BP filter, and the spatial filtering yields a high-quality beam (in terms of collimation and profile) for the objective lens. The Kaiser design is available with a variety of

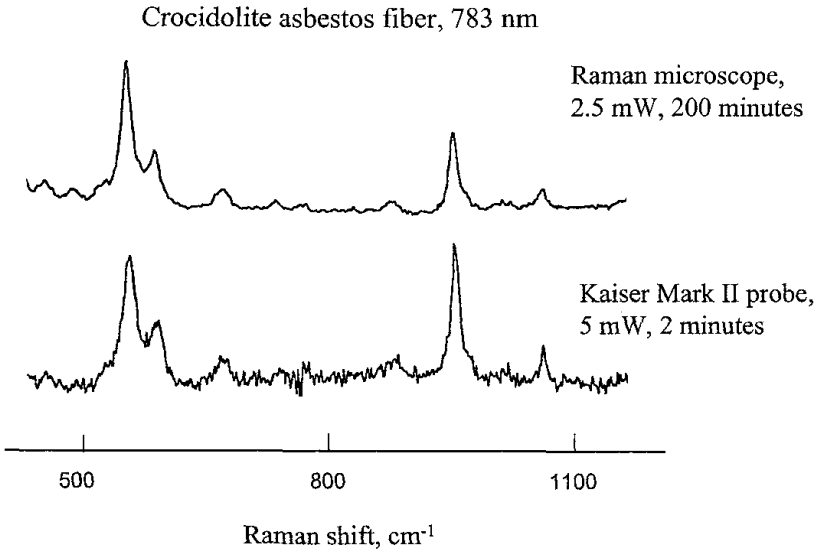

Figure 12.25. Spectra of an asbestos fiber illustrating the focus of a Kaiser Mark II probe. A 2 min acquisition at low power (5 mW) with the fiber-optic probe yielded a useful spectrum that compares well (except for SNR) to a dedicated Raman microscope requiring much longer acquisition time and higher power. (Adapted from Reference 1 with permission.)

focusing lenses and other sampling attachments to interface to a potentially wide range of samples. Figure 12.24 shows spectra of four ribonucleotides in aqueous solution obtained with a Mark II probe (27). The sample was contained in a 50 μm capillary during isotachophoresis, so extremely small quantities of sample were involved (much less than one nanomole). The tight focus of the Mark II was used to advantage to obtain Figure 12.25, a spectrum of a single asbestos fiber. The spectrum is comparable to that from a dedicated Raman microscope. The high noise for the probe is attributable to the much shorter integration time.

12.5. COMPARISONS OF FIBER-OPTIC SAMPLING PROBES

It is clear from previous discussions that fiber-optic probe designs differ substantially in sensitivity, background interference, acceptable fiber length, size, and fragility, not to mention cost. As always, the choice of probe depends on the requirements of the application, so there is no "best" design. Nevertheless, it is useful to address some general comparisons of probe performance.

12.5.1. Probe Figure of Merit

In principle, the signal and signal/noise ratio (SNR) figures of merit discussed in Sections 3.4 and 4.4 can be applied to fiber-optic sampling. Equation (3.11)

defined a figure of merit for a Raman spectrometer that normalized the observed signal for laser power, sample concentration and cross section, and measurement time. One may draw the same distinction between a F'_S [based on total laser power, Eq. (3.11)] and F_S [based on power density, Eq. (3.10)]. As with conventional sampling, probe heads vary significantly in the power density to which the sample is subjected, with possibly large effects on signal and sample radiation damage. A pragmatic approach is to determine a figure of merit empirically by substituting observed parameters for a particular sample into Eq. (12.6), using the variables defined in Section 3.4:

$$F'_S = \frac{S_{\text{obs}}(\text{e}^-)}{P_0 \beta_A D_A t_M} \tag{12.6}$$

The observed F'_S depends on several variables, particularly the fiber numerical aperture, sample depth, interfiber distances, filter losses, and so fourth Similarly, an SNR figure of merit may be determined empirically, which would incorporate SNR degradation due to fiber background. Equation (12.7) for F'_{SNR} is identical to Eq. (4.25), and both are based on experimetnally determined variables:

$$F'_{\text{SNR}} = \frac{\text{SNR}_{\text{obs}}}{(P_0 \beta_A D_A t_M)^{1/2}} \tag{12.7}$$

It is theoretically possible to predict F'_S and F'_{SNR} for different probes, but it is difficult to achieve generality because the results depend on sample properties such as transparency and inelastic scattering efficiency. Nevertheless, for a given type of sample, such as a clear, deep liquid, F_S or F'_S can provide a direct prediction of relative signal strength.

12.5.2. Comparisons of Fiber-Optic Probes

Cooney and co-workers (14,15) performed a detailed theoretical and experimental analysis of probe variations similar to the designs of Figures 12.7, 12.12, and 12.17. These designs do not involve a separate probe head (such as those of Figs. 12.20 and 12.21), but some do involve distal filtering. A figure of merit was calculated for each design, including the n-around-1 probe with flat or beveled tips, and covering a range of fiber diameters and numerical apertures. Their predictions of the dependence of the figure of merit on fiber diameter and interfiber spacing were consistent with those discussed in Section 12.4.1. Several examples are shown in Table 12.2, based on calculations similar to those shown in Figures 12.10 to 12.12. Notice that F'_S increases for the beveled tip over the flat tip due to the increased overlap shown in Figure 12.12. Increased numerical aperture and closer fiber spacing

Table 12.2. Calculated F_S' for Several Probe Designs[a]

Type	Design	Excitation Radius μm	Collection radius μm	Interfiber spacing (center to center) μm	F_S' (relative to type 1)
1	1 around 1[a,b], flat tip	100 (NA = 0.22)	100 (NA = 0.22)	200	1.00
2	1 around 1[a,b], flat tip	100 (NA = 0.33)	100 (NA = 0.33)	200	1.53
3	1 around 1[a,b], flat tip	100 (NA = 0.33)	100 (NA = 0.33)	500	0.63
4	18 around 1	100 (NA = 0.22)	100	—	13.0
5	36 around 1	100 (NA = 0.22)	100	—	18.6
6	1 around 1[a,b], beveled	100	100	200	1.5
7	1 around 1[a,b], beveled	100	100	500	0.83

[a]Data from reference 14, with F_S' assumed to scale with the normalized Raman power of Figure 1 of reference 14.
[b]One excitation fiber, one collection fiber, adjacent and parallel.

also increase F_S'. Not surprisingly, the largest F_S' occurs with multiple collection fibers, such as the 18-around-1 design.

Some valuable experimental results for various probes are shown in Figures 12.26 and 12.27. Seven spectra of an acetaminophen tablet observed by different probes are plotted on the same intensity scale. The observed intensities track the predictions, with larger fibers and beveling resulting in stronger signals. Filtering reduces the signal but has the major benefit of reducing background. In Figure 12.27, the spectra are replotted after normalizing to the intensities of the sample band at ~1300 cm^{-1}. Strong silica features are apparent at ~400 to 600 cm^{-1} for the unfiltered probes. For example, the Carrabba and Rauh design (probe) has about 40 per cent the signal of an unfiltered 6-around-1 design (probe), but the silica background is reduced by a much larger factor, to negligible levels in this case. The trade-off between sensitivity and background rejection is fairly general for fiber-optic probes of the types in general use.

12.5.3. Comparisons of Fiber-Optic Probe Heads

The utility and sensitivity of fiber-optic probe heads are more difficult to compare than those of the fiber-optic probes of Section 12.5.2 because there are a greater number of configurations and variables to consider. Since a

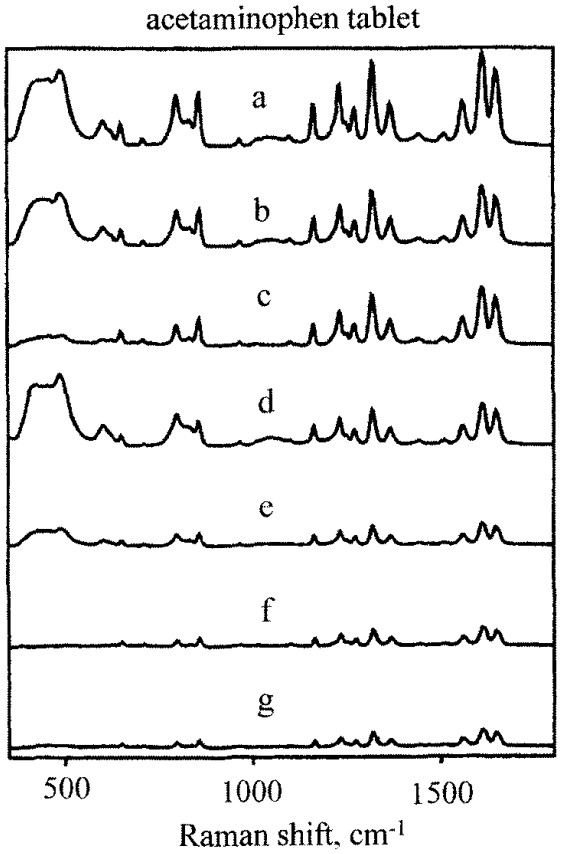

Figure 12.26. Spectra of an acetaminophen tablet obtained with different fiber-optic probes, with the same acquisition conditions and plotted on the same intensity scale. Relative intensities indicate probe efficiency. Probe configurations are: (a) 6 around 1, beveled, 400 μm diameter fibers, unfiltered; (b) 6 around 1 flat tipped, 400 μm, unfiltered; (c) 6 around 1 beveled, 400 μm, filtered; (d) 6 around 1, flat tipped, 200 μm, unfiltered; (e) two-fiber beveled, 400 μm, unfiltered; (f) Carrabba and Rauh design (Fig. 12.17); (g) two-fiber, beveled, 400 μm, filtered. (Adapted from Reference 15, with permission.)

probe head is essentially a 180° sampling system located remotely from the spectrometer, most of the issues discussed in Section 6.3 apply. Probe heads can differ in working distance, laser spot size (and therefore power density), depth of focus, size and number of collection fibers, and the like. A given probe is often modified for samples with varying properties. For example, a longer focal length objective lens may be more sensitive for thick, transparent samples, while a shorter focal length may provide better response for thin, opaque samples. So a comparison of probe heads would need to include several different sample types and optical variables and would probably lose generality. A figure of merit for signal or SNR [as in Eqs. (12.6) and (12.7)] could certainly be defined for probe heads, but any comparisons of such parameters

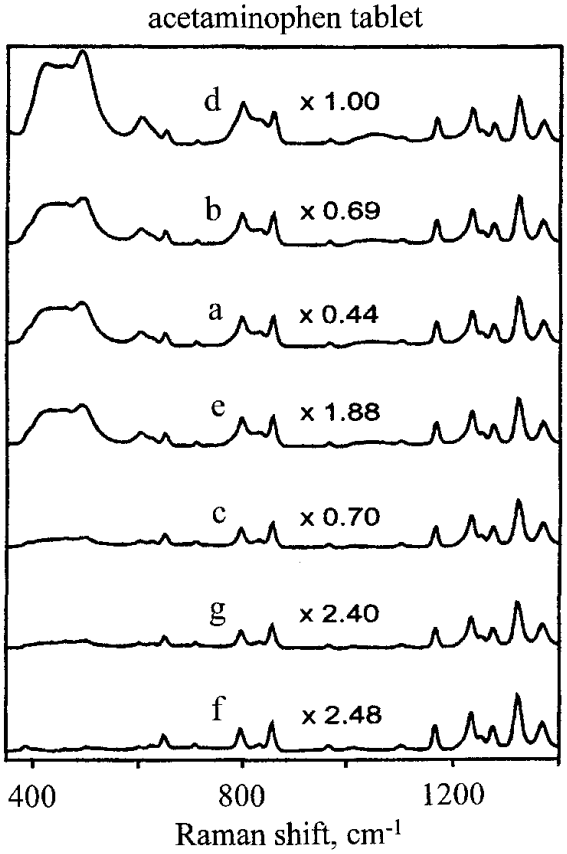

Figure 12.27. Spectra of Figure 12.26 replotted after normalization to the intensity of the 1324 cm^{-1} band. Note the variation of the contribution of the silica features in the 400 to 700 cm^{-1} region for different probe types. The probes are labeled as in Figure 12.26 and ranked according to the degree of silica interference. (Adapted from Reference 15 with permission.)

for competitive head designs would have to precisely specify sample types and acquisition conditions.

That said, there are some useful criteria to consider when evaluating fiber-optic probe heads, including:

1. Physical size
2. Environmental stability (temperature, humidity, etc.)
3. Working distance between probe head and sample and the ability to vary with interchangeable lenses
4. Available laser wavelengths and the ability to change wavelengths (if desired)
5. Provision for polarization analysis (if desired)
6. Laser spot size and its effects on power density and depth of focus

7. Compatibility with spectrometer and laser and ease of alignment
8. Sensitivity to alignment between probe and sample
9. Sensitivity for a given sample type

The sensitivity criterion (item 9) is best evaluated with samples of interest to the user, as sample properties can greatly affect the signal. It is good practice to compare probes in terms of signal per unit of laser power and acquisition time (e.g., in electrons per milliwatt per second, or e^{-} mW^{-1} sec^{-1}) for a given sample. It is usually possible to send particular samples to instrument manufacturers for examination with their probe heads and spectrometers. It is important to know the laser power and acquisition time used by the manufacturer when making such comparisons.

12.6. WAVEGUIDE SAMPLING FOR ANALYTICAL RAMAN SPECTROSCOPY

The term *waveguide* applies to the fiber optic itself but is also used to describe sampling arrangements that modify the interactions between the excitation light, the sample, and the collected light in one of several ways (1,9). In the context of analytical Raman spectroscopy, waveguides have been used to increase sensitivity, localize the measurement spatially, and deal with hostile or difficult sample environments. Several examples will be described in this section, and their potential analytical value will be noted. Throughout the section the term *waveguide* will be used somewhat loosely and is not restricted to phenomena that localize or direct light by total internal reflection. Although there are notable examples of exploiting total internal reflection to localize a measurement to a flat surface (9), the majority of analytical Raman applications use waveguides to increase effective path length for bulk liquid samples in order to increase sensitivity. The discussion below is limited to such cases.

A very early application of a waveguide for Raman spectroscopy occurred in 1972 by Walrafen, who used a tubular fiber optic to contain the sample (28,29). The laser was directed into one end of the tubular fiber optic and the light collected from the other end, then directed into a dispersive/photomultiplier tube (PMT) spectrometer. The sample was chosen to have a refractive index higher than the silica tube, so the laser light and much of the scattered light was totally internally reflected within the tube. The consequence was a very long path length, in the region of several meters, and very high sensitivity. For clear liquids with refractive index greater than silica ($\sim$1.5), strong Raman signals were achieved with a weak He–Ne laser and a spectrometer with much lower sensitivity than a modern dispersive/CCD system.